

Accepted Manuscript

Evaluating the importance of catchment hydrological parameters for urban surface water flood modelling using a simple hydro-inundation model

Dapeng Yu, Tom J. Coulthard

PII: S0022-1694(15)00152-3

DOI: <http://dx.doi.org/10.1016/j.jhydrol.2015.02.040>

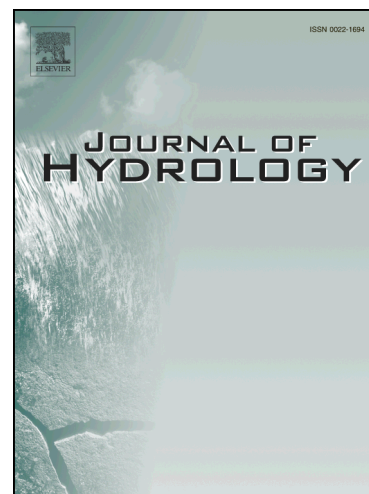
Reference: HYDROL 20283

To appear in: *Journal of Hydrology*

Received Date: 6 October 2014

Revised Date: 19 February 2015

Accepted Date: 21 February 2015



Please cite this article as: Yu, D., Coulthard, T.J., Evaluating the importance of catchment hydrological parameters for urban surface water flood modelling using a simple hydro-inundation model, *Journal of Hydrology* (2015), doi: <http://dx.doi.org/10.1016/j.jhydrol.2015.02.040>

This is a PDF file of an unedited manuscript that has been accepted for publication. As a service to our customers we are providing this early version of the manuscript. The manuscript will undergo copyediting, typesetting, and review of the resulting proof before it is published in its final form. Please note that during the production process errors may be discovered which could affect the content, and all legal disclaimers that apply to the journal pertain.

1 **Evaluating the importance of catchment hydrological parameters for urban surface water flood**
2 **modelling using a simple hydro-inundation model**

3 Dapeng Yu¹ and Tom J. Coulthard²

4 ¹ Department of Geography, Loughborough University, Tel: 01509228191; Fax: 01509223930;
5 d.yu2@lboro.ac.uk

6 ²Department of Geography, Environment and Earth Science, University of Hull

7
8 **Abstract**

9 The influence of catchment hydrological processes on urban flooding is often considered through river
10 discharges at a source catchment outlet, negating the role of other upstream areas that may add to the
11 flooding.. Therefore, where multiple entry points exist at the urban upstream boundary, e.g. during extreme
12 rainfall events when surface runoff dominates in the catchment, a hydro-inundation model becomes
13 advantageous as it can integrate the hydrological processes with surface flow routing on the urban floodplain.
14 This paper uses a hydro-inundation model (FloodMap-HydroInundation2D) to investigate the role of
15 catchment hydrological parameters in urban surface water flooding. A scenario-based approach was
16 undertaken and the June 2007 event occurred in Kingston Upon Hull, UK was used as a baseline simulation,
17 for which a good range of data is available. After model sensitivity analysis and calibration, simulations were
18 designed, considering the improvement of both the urban and rural land drainage and storage capacities.
19 Results suggest the model is sensitive to the key hydrological parameter soil hydraulic conductivity.
20 Sensitivity to mesh resolution and roughness parameterisation also agrees with previous studies on fluvial
21 flood modelling. Furthermore, the improvement of drainage and storage capacity in the upstream rural area is
22 able to alleviate the extent and magnitude of flooding in the downstream urban area. Similarly urban
23 drainage and storage upgrade may also reduce the risks of flooding on site, albeit to a less extent compared
24 to rural improvements. However, none of the improvement scenarios could remove the flow propagation
25 completely. This study highlights that in some settings, urban surface water flood modelling is just as
26 strongly controlled by rural factors (e.g. infiltration rate and water storage) as internal model parameters such
27 as roughness and mesh resolution. It serves as an important reminder to researchers simulating urban
28 flooding that it is not just the internal parameterisation that is important, but also the use of correct inputs
29 from outside the area of study, especially for catchments with a mixture of urban and rural areas.

30

31 **Keywords:** Hydro-inundation model; urban flooding; surface water flooding; pluvial flooding.

ACCEPTED MANUSCRIPT

32 1 Introduction

33 Flood risk managers and decision-makers often face the challenging tasks of designing effective mitigation
34 and adaptation strategies in response to low-frequency and unexpected urban flooding arising from extreme
35 storm events, during which, the combination of surface water runoff and storm sewer surcharge are the two
36 major sources of inundation. Storm sewer flooding is due to the surcharge of excess water that can not be
37 drained by the sewer system and is therefore usually localized. The modelling of storm sewer induced urban
38 flooding has seen a great body of literature in the last few decades, with a range of modelling approaches
39 developed including the 'dual-drainage modelling' (1D/2D) (Djordjević *et al.* 1991; Hsu *et al.* 2000; Schmitt
40 *et al.* 2004) and the 1D/1D approach (Mark *et al.* 2004). Such approaches typically couple: (i) the solution of
41 the 1D shallow water equations for the storm sewer systems; and (ii) a 1D or 2D representation of surface
42 flow. These approaches are able to provide a good estimate of urban flood risks at the local scale. The
43 accuracy of the model predictions depends on a number of factors, including the accuracy of: (i) the
44 topographic data; (ii) inflow to the drainage inlets, usually derived from hydrological estimation; and (iii) the
45 geometries of the storm sewer pipes. In comparison, direct surface water runoff in urban environments are
46 less well studied. Surface water flooding may arise from rainfall-generated overland flow before the runoff
47 enters watercourses or is captured by the sewer system. It is usually associated with high intensity rainfall
48 (e.g. >30 mm/hour), during which urban storm sewer drainage systems and surface watercourses may be
49 overwhelmed, preventing drainage through artificial (e.g. pumping) or natural means (e.g. gravity).
50 Moreover, even when fully functioning, urban storm sewer systems may not have the capacity to capture all
51 the surface runoff through inlets during extreme events and direct surface runoff can overpass manholes and
52 accumulate to form ponding in topographic depressions due to inlet efficiency (Aronica and Lanza 2005). In
53 addition, surface water flooding can also originate from rural areas adjacent to the urban settlements where
54 extreme rainfall runoff accumulates along flow paths without being captured by the land drainage/storage
55 systems. Recently, 2D surface flow routing models have been used to simulate the urban surface water
56 runoff originating from point sources (e.g. manholes), using synthetic or model-derived flow hydrographs
57 (e.g. Mignot *et al.* 2006; Fewtrell *et al.* 2011). In these studies, the interaction between surface runoff and
58 storm sewer is either considered as insignificant, or represented through a mass loss term determined based
59 on the drainage capacity. Modelling 2D surface water runoff in urban catchment is challenging due to the
60 needs to consider both the hydrological (e.g. precipitation, infiltration and evapotranspiration) and hydraulic

61 processes (surface flow routing), in a topographically complex environment. The representation of
62 spatiotemporal variation in precipitation, and effect of land characteristics (e.g. land use and soil type) is
63 required for the former in order to calculate the right amount of rainfall runoff, while high-accuracy
64 topographic data where topographic connectivity is preserved is essential for routing the surface runoff to the
65 correct places.

66

67 More recently, researchers have incorporated direct precipitation into 2D flow routing models in urban
68 environments. Such models can be termed as “hydro-inundation models” whereby hydrological processes are
69 considered simultaneously with floodplain flow routing. Hydrological and inundation processes are two
70 interlinked processes but they have so far been largely investigated in isolation, with hydrological outputs at
71 the catchment-scale used as inputs to surface flow routing at the upstream boundary. Linking these two sub-
72 systems using a unified hydro-inundation model is a logical step towards integrated modelling, especially
73 when multiple entry points exist at the catchment/floodplain boundary. The use of a hydro-inundation model
74 is particularly advantageous for decision makers to evaluate the impact of catchment-wide hydrological
75 processes on urban flood inundation. The role of land management scenarios (e.g. improved storage capacity
76 and improved drainage) can be tested using such models. Whilst commercial software packages already offer
77 such functions, represented by the surface water flood map produced by the EA (EA, 2013), research studies
78 coupling hydrological and inundation processes are rare, especially in urban areas. Chen *et al.* (2009) used a
79 nested approach to incorporate hourly rainfall on a 5 km grid upstream in the upstream catchment and a finer
80 rainfall field of 15-minute on a 2 km grid for hydraulic modelling in the downstream. A non-inertial model
81 was used (URM, Chen *et al.* 2007) and the focus was placed on filtering rainfall events and considering
82 future climate change scenarios derived from UKCP09 predictions. Sampson *et al.* (2013) presented a
83 modelling study of surface water flooding at a local scale (0.5 km^2) with a uniform rainfall input and a
84 synthetic single point culvert surcharge using a flood inundation model (LISFLOOD-FP), focusing on: (i)
85 routing rainwater from elevated features; and (ii) comparison with commercial modelling packages.
86 Hydrological factors (e.g. infiltration and evapotranspiration) were not considered due to the solely urban
87 nature of their study site, and validation was not undertaken due to limited data availability. In this study, we
88 describe the application of a hydro-inundation model (FloodMap-HydroInundation2D) to investigate the
89 importance of urban and rural land drainage/storage capacity on flood inundation in catchment with a

90 mixture of urban and rural areas, using the June 2007 event in the city of Kingston upon Hull, UK as the
 91 baseline simulation.

92

93 2 Methods

94 2.1 The hydro-inundation model used

95 The model (FloodMap-HydroInundation2D) is developed based on the modified version (local inertial-based)
 96 of FloodMap (Yu and Lane 2006a), which is a two-dimensional flood inundation model designed for
 97 modelling flood inundation over topographically complex floodplains. The model has been tested and
 98 verified with a range of boundary conditions and in a number of environments (Yu 2005; Yu 2010; Tayefi *et al.*
 99 *et al.* 2007; Lane *et al.* 2008; Casas *et al.* 2010; Yin *et al.* 2013). It is modified to incorporate the key
 100 hydrological processes during an urban storm event into surface flow routing, including infiltration and
 101 evapotranspiration.

102

103 2.1.1 Surface flow routing

104 The 2D flood inundation model (FloodMap-Inertial) takes the same structure as the inertial model of Bates *et al.*
 105 *et al.* (2010), but with a slightly different approach to the calculation of time step. Neglecting the convective
 106 acceleration term in the Saint-Venant equation, the momentum equation becomes:

$$107 \quad \frac{\partial q}{\partial t} + \frac{gh\partial(h+z)}{\partial x} + \frac{gn^2q^2}{R^{4/3}h} = 0 \quad (1)$$

108 Where q is the flow per unit width, g is the acceleration due to gravity, R is the hydraulic radius, z is the bed
 109 elevation, h is the water depth and n is the Manning's roughness coefficient. Discretizing the equation with
 110 respect to time produces:

$$111 \quad \frac{q_{t+\Delta t} - q_t}{\Delta t} + \frac{gh\partial(h+z)}{\partial x} + \frac{gn^2q_t^2}{h_t^{7/3}} = 0 \quad (2)$$

112 To further improve this, one of the q_t in the friction term can be replaced by $q_{t+\Delta t}$ and this gives the explicit
 113 expression of the flow at the next time step:

$$114 \quad q_{t+\Delta t} = \frac{q_t - gh_t\Delta t\left(\frac{\Delta(h_t+z)}{\Delta x}\right)}{\left(1 + \frac{gn^2\Delta t q_t}{h_t^{10/3}}\right)} \quad (3)$$

115 The flow in the x and y directions is decoupled and take the same form. Flow is evaluated at the cell edges
 116 and depth at the centre.

117

118 FloodMap evaluates the flow directions in x and y for each pixel at each iteration based on the orthogonal
 119 slopes. The flow rate across a cell boundary is calculated using (3) for the two directions associated with the
 120 greatest orthogonal slope. Therefore, only positive flow is allowed in each direction. Net inflow is calculated
 121 for each pixel based on total inflow and outflow which can then be used to update water depth for the time
 122 step. Instead of using a global Courant-Freidrich-Levy Condition (where the time step for the next iteration is
 123 calculated based on the maximum water depth and velocity found at the last time step e.g. Bates and De Roo
 124 2000; Yu and Lane 2006a), the Forward Courant-Freidrich-Levy Condition (FCFL) approach described in
 125 Yu and Lane (2011) for the diffusion-based version of FloodMap is used in the inertial model to calculate
 126 time step. The maximum time step that will satisfy the CFL condition for a given wet cell is calculated as:

$$127 \quad \Delta t_{i,j} \leq \frac{w \times n \times (S_i^2 + S_j^2)^{1/4}}{d^{0.67} (S_i + S_j) + \sqrt{g \times D \times n \times (S_i^2 + S_j^2)^{1/4}}} \quad (4)$$

128 where w is the cell size, d is the effective water depths, S_i and S_j are water surface slopes, and i and j are the
 129 indices for the flow direction in the x and y direction respectively. The effective water depth is defined as the
 130 difference between the higher water surface elevation and the higher bed elevation of two cells that exchange
 131 water. The minimum time step that satisfies the FCFL condition for all the wet cells is used as the global
 132 time step for this iteration. Comparison with the ATS scheme using the analytical solution of floodplain
 133 wetting over a horizontal plane used by Hunter et al. (2005), the FCFL condition was found to be less
 134 constraining due to the lower exponent (0.67 as opposed to 1.67) on effective water depth in the denominator
 135 (Yu and Lane 2011). As the FCFL condition is not strictly the right stability criteria for an inertial system,
 136 this scheme still may not guarantee a stable solution, and thus may still produce unrealistic wave propagation.
 137 The universal time step calculated with FCFL may need to be scaled further by a coefficient, the value of
 138 which ranges between 0 exclusive and 1 inclusive. A scaling factor of 0.5-0.8 was found to give stable
 139 solution to all the simulations carried out in this study and a scaling factor of 0.7 was used in all the
 140 simulations undertaken.

141

142 2.1.2 Infiltration and Evapotranspiration

143 Infiltration over saturation is represented by the widely used Green-Ampt infiltration equation, which
 144 approximates the rate of infiltration as a function of the capillary potential, porosity, hydraulic conductivity
 145 and time, taking the following form:

$$146 f(t) = K_s \left(\frac{\varphi_f + h_o}{z_f} + 1 \right) \quad (5)$$

147 Where K_s is the hydraulic conductivity of the soil at field saturation, φ_f is the capillary potential across the
 148 wetting front, h_o is the ponding water on the soil surface, and z_f is cumulative depth of infiltration.
 149 Hydraulic conductivity is often used as a calibration parameter in hydrological studies.

150

151 Evapotranspiration is calculated using a simple seasonal sine curve for daily potential evapotranspiration
 152 (Calder *et al.* 1983) with the equation below:

$$153 E_p = \overline{E_p} \left[1 + \sin \left(\frac{360i}{365} - 90 \right) \right] \quad (6)$$

154 Where $\overline{E_p}$ is the mean daily potential evapotranspiration and i is the day of the year.

155

156 For hydro-inundation modelling, the amount of evapotranspiration during storm and flooding
 157 conditions is in the order of 3-5 mm/day, a small amount compared to infiltration and drainage
 158 processes.

159

160 2.1.3 Drainage capacity in urban areas

161 Mass loss to the storm sewer system is considered in the model by its design capacity, usually corresponding
 162 to a rainfall event of certain intensity (mm/h) and return period. If the model is applied to an extreme event
 163 (defined here as a > 1 in 100 year), it is reasonable to assume that the storm sewer system drains water away
 164 at the maximum design capacity. For each time step, the amount of runoff loss to the urban storm sewer
 165 systems is calculated by scaling the drainage capacity (mm/hour) for the time step. Distributed drainage
 166 capacity also can be incorporated into the model on a cell by cell basis. However, manholes and drains are
 167 not explicitly represented in the model (e.g. Liu *et al.* 2014). Rather, the drainage capacity is considered as a
 168 lump value that operates over a specific area, draining to its design capacity throughout that whole area.

169

170 **2.2 Study site and the event**

171 The city of Kingston upon Hull (hereafter Hull) is located on the River Hull at its junction with the Humber
172 estuary. The terrain of the city itself is low-lying, with ground elevation ranging between 2 m to 4 m AOD.
173 The mean sea level in the East coast of the UK is above AOD and the Humber estuary experiences a tidal
174 range of c.6m. Therefore, over 90% of the city is below the high tidal level. Until the mid 1960's, a system
175 of open drains and tidally operated gates drained the city, but these were replaced with a combined sewage
176 and drainage system evacuated by three large pumping stations. As a result, the drainage system for the city
177 of Hull is entirely pumped (Coulthard and Frostick, 2010). The city is protected from tidal inundation by
178 embankments and flood walls along the estuary and by a tidal barrier operating on the River Hull to prevent
179 the progression of high tides up the river that dissects the city. Following the modernisation of the drainage
180 system in the 1960's and prior to 2007, significant fluvial and coastal flooding has been absent from recent
181 history although it is anticipated that sea level rise and increased storminess might be increasing the risks of
182 coastal flooding. In 2007, the city experienced widespread flooding from a pluvial event for >>12 hours,
183 totalling 110 mm. The 25th June 2007 24-hour rainfall is estimated to be a one in 150 year (CEH Flood
184 Estimation Handbook; Yorkshire Water pers. comm., Coulthard and Frostick 2010) and greater than 1 in 200
185 years by Hanna *et al.* (2008). Antecedent conditions were wet due to a 1 in 30 year event ten days
186 previously. The 25th June flooding caused damage to over 8600 residential and 1300 businesses, and flooded
187 over 600 roads (Coulthard *et al.* 2007a). During the event, water was contained in the River Hull and it was
188 reported that only the Setting Dyke, which is an open drain to the west of the city overtopped briefly
189 (Coulthard *et al.* 2007a). Groundwater was greatly elevated but it was not found to cause flooding during this
190 event. The major cause of the flooding is surface water runoff (Halcrow 2009) both locally in the urban area
191 and through the rural lands surrounding the city. Hull has a storm sewer system with a design standard of 1
192 in 30 years (70mm/day, Coulthard *et al.* 2007a). However, due to the sheer magnitude of the 2007 event,
193 although fully functioning during the event, the storm sewer system was overwhelmed and unable to drain
194 the excess surface runoff. This event has prompted the suggestion that, for a low-lying coastal city such as
195 Hull, a one in 30-year storm sewer system is insufficient, especially in the wake of the potential climate
196 change and variability (Coulthard *et al.* 2007b). In this study, we focus on the worst hit areas to the west of
197 the city (Figure 1) where surface runoff was found to be the most severe.

198

199 *Figure 1*

200

201 **2.3 Data availability and processing**202 **2.3.1 Topographic data**

203 Elevation data in Hull is available in the form of a high resolution (1 m) LiDAR dataset, processed by the
204 UK Environment Agency's National Centre for Environmental Data Surveillance in Twerton, Bath, to a
205 vertical precision of +/- 25 cm throughout, and +/- 15 cm in low relief areas with solid reflectance surfaces.

206

207 **2.3.2 Precipitation data**

208 Within and in the vicinity of Hull, six rainfall gauging records are available from the UK Met Office and
209 Hull University, but only one is in the city itself. The rainfall hyetographs of the stations are shown in Figure
210 2, demonstrating the spatial and temporal heterogeneity of precipitation in the records. The 24-hour
211 precipitation total ranges between 51.6 mm (Cottingham) and 119.6 mm (Winestead). Considering the
212 degree of consistency within the data records, the gauging data at the Hull University (total 110 mm) was
213 used in the modelling. It should be noted that this rainfall record is un-calibrated, and using data from a
214 single site is likely to introduce uncertainties into the representation of rainfall spatiotemporal characteristics.
215 However, given the size of the study site and the scenario-based nature of the modelling approach, this is
216 considered adequate.

217

218 *Figure 2*

219

220 **2.3.3 Observed inundation**

221 A set of observation data describing the inundation extent of the event is available, including: (i) the extent
222 of inundated areas provided by the UK Environment Agency and the Hull City Council, consisting of
223 information derived from various sources including ground survey and aerial photos; and (ii) buffer of
224 houses flooded provided by the Hull City Council. The observation data within the study area are shown in
225 Figure 3. Water depths are reported to be up to 3 m locally, but for most areas affected the depth is less than
226 1m and many properties were flooded less than 50 cm (Coulthard and Frostick 2010).

227

228 *Figure 3*

229

230 **2.4 Simulation design**

231 Digital Terrain Models (DTMs) of two resolutions (10 m and 20 m) were produced to test model sensitivity
232 to topographic resolution. The total number of pixels in each DTM is 0.9 million and 0.2 million respectively,
233 indicating the quadratic increase of the computational resources required with the fining of mesh resolution.

234

235 Roughness and hydraulic conductivity are the key parameters for model calibration. An initial screening was
236 undertaken to constrain the possible range of values for these two parameters in simulating this particular
237 flood event. A hydraulic conductivity (K_s) value of between 0.001 m/h and 0.005m/h was found to produce
238 reasonable model response. Further justification to the choice of K_s values is provided in Section 3.2 where
239 model calibration is discussed. Model sensitivity to roughness parameterisation is evaluated by varying the
240 Manning's n value (0.01, 0.02, 0.03, 0.04 and 0.05), while keeping the hydraulic conductivity at 0.005 m/h.
241 The default drainage capacity of the urban areas takes the design drainage capacity of the city, i.e. 70
242 mm/day, and that of the rural areas is set as 15 mm/day, based on the typical design capacity of 10 mm/day
243 widely used in the lower rainfall areas of the UK (Trafford, 1971). This, in combination with the mesh
244 resolution, generates 15 simulations, allowing the model response to mesh resolution and roughness
245 parameterisation to be investigated.

246

247 Land drainage and storage capacity affects the amount of surface runoff that in turn may cause flooding.
248 Improving the drainage and storage capacity through rural land management (e.g. tilting, piping and ponds)
249 and urban drainage improvement (e.g. storm sewer retro-fit, SuDS, aqua-green and underground storm water
250 storage) may result in reduced amounts of surface runoff. After testing the model sensitivity to mesh
251 resolution and calibration with roughness and hydraulic conductivity parameters, simulations were designed,
252 accounting for various urban and rural drainage and storage capacities and their combinations. Urban (80%)
253 and rural (20%) areas were delineated based on the Ordnance Survey MasterMap dataset. Drainage and
254 storage improvement scenarios were designed by considering: (i) an increase of urban drainage and storage
255 capacity to 120 mm/day at a 10 mm interval (i.e. 80 mm, 90 mm, 100 mm, 110 mm and 120 mm); and (ii)

10

256 improvement of rural drainage/storage capacity up to 115 mm/day at a 20 mm interval (i.e. 35 mm, 55 mm,
257 75 mm, 95 mm and 115 mm). These are summarized in Table 1. It is noted that the values of drainage and
258 storage improvement are rather optimistically designed if we consider typical drainage capacity alone (e.g.
259 30 mm/h). However, for both urban and rural environments, there is scope for innovative and ‘extreme’
260 storage improvement (e.g. Water Plazas and underground storm water storage) which will render the above
261 design drainage and storage feasible.

262

263 It should be recognized that the impact of rural land drainage on river peak flow is highly uncertain and
264 likely to be site specific, depending on the soil type, antecedent conditions and rainfall event (Blanc *et al.*
265 2012 and Robinson 1990). Interested readers could refer to the studies by Robinson (1990) and Blanc *et al.*
266 (2012) for extensive review on the impact of land drainage. As we focus on surface water flooding, measures
267 that improve land drainage and storage capacity are likely to exert a positive effect as it reduces surface
268 runoff. However, it is uncertain whether such improvement will aggravate fluvial flooding.

269

270 *Table 1*

271

272 **3 Results**

273 **3.1 Sensitivity to roughness and mesh resolution**

274 Model sensitivity to the roughness parameter is evaluated by varying the Manning’s n value (0.01, 0.02, 0.03,
275 0.04 and 0.05). Figure 4 demonstrates the model response to the variation and in terms of inundation extent
276 (Figure 4a), the model responds as expected for individual mesh resolution, with a higher roughness value
277 slowing flood propagation. An n value of 0.01 produces the largest inundation in all cases. However,
278 inundation extent differs only marginally for n values between 0.02 and 0.05, suggesting that in this
279 application the model is relatively insensitive to roughness specification. F statistic and RMSE (Figures 4b
280 and 4c) compare the temporal difference between the spatial distribution of inundated areas and water depths
281 for simulations with an n value of 0.02, 0.03, 0.04 and 0.05 using the 0.01 simulation as the reference for each
282 mesh resolution. The model becomes more sensitive when evaluated against F statistic and RMSE,
283 demonstrating the spatial and temporal variability of the predicted wetted area and depth distribution.

284

285 After a brief peak, the F statistic drops to a rather low level, suggesting a mismatch in the predicted
286 inundated areas during the initial wetting process. However, when the timing (8th hour) of the F statistic peak
287 is cross-examined with the total inundation area (Figure 4a), it can be seen that this peak is associated with
288 minor wetted area. The F value gradually picks up with the onset of surface runoff. As the peak inundation
289 occurs (c. 16:00), the F statistic reaches the highest. Model's sensitivity to roughness when evaluated using F
290 statistic suggests the varying flow velocity associated with different roughness values.

291

292 The magnitude of RMSE is relatively small (< 2.5 cm) in all cases and varies over time and is a function of
293 the roughness value. However, it should be noted that the RMSE is the aggregated depth variation from the
294 base simulation ($n=0.01$) over the study area at a particular time. Therefore, the spatial distribution of depth
295 difference is not considered explicitly. Spatial variation of the depth prediction is expected and this will be
296 illustrated further.

297

298 *Figure 4*

299

300 Figure 5 explores the model sensitivity to mesh resolution also considering the roughness parameters. When
301 the total inundation area is evaluated over time, the model is relatively insensitive to mesh size during the
302 rising limb and demonstrates a certain degree of sensitivity during the falling. However, the sensitivity to
303 mesh resolution is also a function of the roughness parameter, as roughness value increases the sensitivity
304 decreases. Sensitivity is also reflected in the F statistic, however, the correlation between mesh resolution
305 and roughness becomes notably weaker when the F statistic is used. There is a slight increase in the
306 sensitivity with the increase of roughness value when F is considered. RMSE response is more complex, but
307 consistent for n values of 0.03, 0.04 and 0.05. As F and RMSE are relative metrics, calculated against the
308 reference simulation with an n value of 0.01 for respective mesh resolution, comparing these for different
309 resolutions might not reveal the sensitivity.

310

311 *Figure 5*

312

313 **3.2 Model calibration and validation**

314 Given the marginal difference in the model sensitivity to mesh resolution when peak inundation is
315 considered (Figure 4a) and accounting for computational efficiency, the 20 m DTM is used in the subsequent
316 simulations. Manning's n is kept at 0.03, a value in the theoretical range of roughness specification. Whilst a
317 uniform roughness value of 0.03 simplifies the representation, given the scenario-based nature of this study,
318 it is regarded as an adequate assumption.

319

320 Due to the uncertainties in rainfall representation and drainage and storage capacity (both rural and urban),
321 soil hydraulic conductivity (K_s) was used as a calibration parameter. This compensates for the simplified
322 representation of rainfall and drainage/storage capacity and aims to produce the optimal match with the
323 observation data for the base simulation.

324

325 Soil hydraulic conductivity can be determined either use empirically-based correlation methods or through
326 in-situ hydraulic laboratory measurements. The latter is practically infeasible for urban catchments. We use
327 empirically-based methods to estimate soil hydraulic conductivity in West Hull. Such methods typically
328 associate K_s with soil properties (texture, pore-size and grain size distribution) or soil mapping units
329 (Oosterbaan and Nijland 1994). Surface deposit in Hull is characterised by alluvium and tidal flat deposits
330 comprising of clay and silt, and major soil types include stony, silty or clay loams, characterised by fine silty
331 material overlying lithoskeletal chalk usually occurring in well-drained areas (O'Donnell *et al.* 2004). The
332 K_s value for the study site is therefore determined based on the lower range of the typical K_s suggested by
333 Smedema and Rycroft (1983) and through a calibration process, during which Fit statistic is used to evaluate
334 the match in extent between the model prediction and observation (Figure 3). The final set of K_s values
335 tested include 0.001, 0.002, 0.003, 0.004 and 0.005 (m/h), covering the lower range of the K_s values
336 suggested by Smedema and Rycroft (1983), reflecting the urbanized nature of the catchment. The results are
337 shown in Figure 6.

338

339 The model was found to be very sensitive to the specification of hydraulic conductivity (Figure 6) and a
340 small variation of this parameter results in a notable change in the amount of infiltration (Figure 6b) and
341 extent of inundation (Figure 6a). The simulation with a K_s value of 0.001 is used as the reference simulation

342 and RMSE and F are calculated over time. RMSE and F statistic (Figures 6c and 6d) also demonstrate the
343 spatiotemporal variation of model predictions.

344

345 *Figure 6*

346

347 Furthermore, we decouple the main hydrological components into total rainfall, infiltration loss,
348 evapotranspiration loss and drainage loss to evaluate the temporal changes in water balance in Figure 7.

349

350 *Figure 7*

351

352 Model validation aims to reproduce the extent of inundation that best approximates the observed extent in
353 the worst-hit areas, i.e. the urban areas adjacent to the rural lands to the west of the city. A hydraulic
354 conductivity value of 0.003 m/h was found to produce the best match, with an overall F value of 35%. It
355 should be noted that given the nature of surface water flooding, the observed data are likely to underestimate
356 the extent of flooding, especially for isolated patches of flooded area. Indeed, the inundation extent collated
357 by the EA and Council differs to a large extent (Figure 3). Therefore the relatively low F value may not be a
358 good indication of the model performance. This will be further evaluated in section 4.2. The time series of
359 inundation is shown in Figure 8. The temporal sequence of inundation is reproduced well in the simulation.
360 Excess water that cannot be drained away due to the limited urban and rural drainage capacity is routed to
361 the topographic lows and accumulates to the edge of the urban areas following topographic gradients (10:00
362 Figure 8). Water then enters the worst-hit regions and propagates further into the city centre (12:00 Figure 8).
363 Water starts to recede at around 16:00 but there remain areas of inundation until late in the day (22:00
364 Figure 8).

365

366 *Figure 8*

367

368 **3.3 Effects of improved urban drainage and storage capacity**

369 One immediate question following this significant flood event is whether improved urban drainage capacity
370 through pumping could alleviate its impact. The Final Independent Report (Coulthard *et al.* 2007) on the

371 flood recommended that designs based on industry standards to protect from a 1 in 30 years storm event may
372 not be adequate and additional capacity should be considered due to potential climate change and variability.
373 The Interim Independent Report (Coulthard *et al.* 2007) commissioned by the City Council suggested that to
374 slow down the addition of water to the drainage systems, temporary reservoirs could be created. Strategic
375 interception of surface water could also be considered for routing the excess water to storage areas. In the
376 council's Surface Water Management Plan, similar measures are suggested (Hull Council 2009).

377

378 We undertook simulations to evaluate the potential impact of improved drainage and storage capacity in the
379 urban areas. Urban drainage and storage improvement scenarios consider capacity increase from the current
380 70 mm/day to 120 mm/day at a 10 mm interval. The total inundated area is shown in Figure 9a for the
381 baseline simulation and the scenarios. This is shown in comparison with the combination of: (i) a medium
382 improvement of urban and rural drainage/storage to 100 mm/day and 75 mm/day respectively (dotted red
383 line); and (ii) the optimal improvement of urban and rural drainage/storage to 120 mm/day and 115 mm/day
384 respectively (solid red line). The predicted extent for each scenario over time is compared to the baseline
385 simulation using the Fit statistic and this is shown in Figure 9b. Figure 9c shows the global derivation over
386 time for the depth prediction in each scenario compared to the baseline simulation. As expected, the total
387 inundated area decreases with the improvement of drainage capacity. An increase to 120 mm/day results in a
388 marked reduction (40%) of the peak inundation extent from the default simulation. This is also reflected in
389 the F statistic.

390

391 *Figure 9*

392

393 In terms of the predicted water depth, although the magnitude of RMSE (overall deviation from the default
394 simulation) is relatively small (Figure 9c), the spatial distribution of the depth difference suggests big
395 variations in the reduction magnitude across the study area (Figures 9). The difference is localized in places
396 where water depth is high in the default simulation.

397

398 *Figure 10*

399

400 Water depth over time is plotted (Figure 11) for: (i) discrete points along the two main flow pathways
401 leading to the urban areas (P1-P5 and P6-P10); (ii) one point at the edge of the urban area (P11); and (iii) one
402 point in the city centre (P12). Among the points, P2 and P11 are located in rural areas. Points 1-5, and points
403 6-10 follow the two main flow pathways leading to the worst-hit areas respectively. Depth profiles
404 demonstrate the rapid response to precipitation in the headwaters (P1, P2, P6 and P7), during both the rising
405 and falling limbs of the flood event. Water depth rises fast in the worst-hit areas but the receding phase is
406 prolonged as water accumulates to the local topographic lows (P3, P4, and P10). As expected, the urban
407 drainage capacity does not directly affect the point depths in the rural areas (P11), except for places that
408 urban water feeds to (P2). Sensitivity to urban drainage/storage capacity is more pronounced for points in the
409 city centre where water accumulates (P3, P4, P5, P10 and P12).

410

411 *Figure 11*

412

413 **3.4 Effects of improved rural land drainage and storage**

414 Surface water runoff from rural land adjacent to the urban settlement is the major source of flooding for
415 West Hull during the event. Upgrading the urban drainage and storage capacities may reduce flooding in the
416 city centre itself. However, it will not affect the amount of water entering the city from the adjacent rural
417 land to the west. Intercepting surface runoff from rural land is seen as a potentially useful measure for
418 managing surface flood risks in Hull (Coulthard *et al.* 2007; Hull Council 2009). Modelling work undertaken
419 in the Council's Surface Water Management Plan suggests that preventing overland flow entering the urban
420 area by means of embankments or walls could have significant benefits. Two options were explored
421 including an embankment to the west of A164 and using a golf course adjacent to the city centre as storage
422 area in conjunction with an embankment (Figure 3). Apart from creating temporary water storages on the
423 floodplain, improving land drainage and storage capacity could also be considered in conjunction with other
424 options. Instead of assessing the effectiveness of individual/combined options, we focus on their net impact
425 on the total amount of water entering the urban areas. In this way, the combined impact of measures taken in
426 the rural areas is simplified into a reduced amount of floodwater entering the urban area from various entry
427 points (Figure 8). In a similar way to the investigation of urban drainage and storage capacity, the potential
428 impact of improved rural land drainage and storage capacity was evaluated, based on five improvement

429 scenarios from 15 mm/day to 115 mm/day at a 20 mm interval. The comparison with the default simulation
430 is shown in Figure 12, alongside with the combination of: (i) a medium improvement of urban and rural
431 drainage and storage to 100 mm/day and 75 mm/day respectively; and (ii) the optimal improvement of urban
432 and rural drainage and storage to 120 mm/day and 115 mm/day respectively.

433

434 *Figure 12*

435

436 The reduction of maximum water depth with an improved rural land drainage and storage capacity from 15
437 mm/day to 55 mm/day and 115 mm/day is shown in Figures 11a and 11b respectively. A moderate
438 improvement to 55 mm/day results in notable reduction of water depth, especially in the Derringham area
439 (Figure 3). The difference becomes much more pronounced when the drainage and storage capacity of the
440 rural land is increased to 115 mm/day.

441

442 *Figure 13*

443

444 The point depth profiles over time are shown in Figure 14 for different drainage and storage improvement
445 scenarios. The patterns are as expected but none of the scenarios result in substantially reduced water depth
446 for the points investigated, except point 5.

447

448 *Figure 14*

449

450 **4 Discussion**

451 **4.1 Sensitivity analysis and model calibration**

452 Model sensitivity to mesh resolution and roughness parameter reveals an interesting model response in
453 comparison to studies in fluvial flood modelling. Yu and Lane (2006a) reported greater inundation with a
454 coarser mesh, for a relatively urban site with extended but laterally confined floodplain. In an application to a
455 small urban district considering surface flooding due to sewer surcharge, Ozdemir *et al.* (2013) found that a
456 finer mesh allows water to propagate along “channels” that form at the road edge, thus resulting in greater
457 inundation. The former finding can be explained by the simplified nature of a diffusion-based inundation

458 model, while the latter is associated with the degree of details in the representation of urban features that
459 control flow propagation. With the additional consideration of hydrological processes such as precipitation,
460 infiltration and evapotranspiration, the surface flow routing demonstrates various degrees of sensitivity to
461 mesh resolution and roughness parameter when evaluated against different metrics. The sensitivity is
462 therefore two-fold. On one hand, the model is rather insensitive to varying mesh sizes and roughness values
463 (Figure 4 and Figure 5), when the inundation area is considered. On the other, the spatial metrics (i.e. F and
464 RMSE) demonstrate much greater degree of spatial/temporal variability in the prediction than the global
465 metric (i.e. total inundated area), suggesting model's sensitivity to mesh resolution and roughness
466 specification. Figure 15 shows the prediction of maximum water depth reached for the whole study area and
467 in a subset, for the 5 m, 10 m, 50 m and 100 m mesh respectively. The "channel" effect exerted by a finer
468 mesh reported in Ozdemir *et al.* (2013) can be confirmed from this. As the inertial model used in this study
469 differs from Yu and Lane (2006a) due to the additional consideration of momentum terms in the governing
470 equation, the response to mesh resolution might change and future studies could be undertaken to explore
471 any difference.

472

473 Figure 15 also illustrates the deterioration in the details of prediction if a 50 m or 100 m DEM is used in the
474 simulation. Systematic evaluations of the sensitivity to roughness and mesh resolution for fluvial flood
475 inundation models have been undertaken in previous studies (e.g. Yu and Lane 2006a; Ozdemir *et al.* 2013).
476 However, as hydro-inundation modelling is relatively new, studies in this area are rather limited. This study
477 focuses on finer meshes for an urban site. Future studies could be directed to evaluate DEM of various mesh
478 resolution and in a range of environments, to better understand the interaction between roughness
479 parameterisation and topographical representation.

480

481 *Figure 15*

482

483 Model calibration shows that the model is highly sensitive to soil hydraulic conductivity (K_s). With a 0.001
484 m/h decrease of K_s , an average increase of 1.65 sq. km of peak inundated area is predicted (Figure 6a). This
485 is due to the amount of reduced infiltration associated with a smaller hydraulic conductivity value (Figure
486 6b). Global metric RMSE shows notable difference between simulations (Figure 6c) and spatial comparison

487 (F) of extent shows a similar trend (Figure 6d). The water balance profiles shown in Figure 7 corroborate
488 those in Figure 6, suggesting that the model is highly sensitive to hydraulic conductivity, a key parameter in
489 model calibration.

490

491 **4.2 Model evaluation and uncertainty analysis**

492 Although reconstruction of the flooding temporal sequence proved to be difficult due the fast-developing
493 nature of surface water flooding and the challenges in accounting for the temporal and spatial dynamics,
494 discrete information on the timing of flooding is available from various sources. The Hull City Council
495 reported that, from 6:00 am, calls for emergency assistance quickly reached a peak of around 100 an hour
496 and this level were sustained till 9:00 pm, with a Major Incident being declared at 09:30 am. In terms of the
497 operation of the drainage system, it was reported that the inlet penstocks to West Hull Pumping Station
498 were opened at approximately 7:00 am. Between 8:00 am and 8:15 am, the levels in the sumps for West
499 Hull pumping station rose by 6 m from approximately -1 m (Coulthard *et al.* 2007), indicating when water
500 discharged into the pumping station wells and the pumps started. It is likely that the sewers in West Hull
501 were fully surcharged when the pumps in West Hull started (Coulthard *et al.* 2007). The temporal
502 information available agrees in general with the model predictions (Figure 8). However due to the resolution
503 of the information, a statistical evaluation is not possible.

504

505 Comparisons between model predictions and observation data prove challenging due to the uncertainties in
506 both. Observation data are likely to be incomplete and uncertain due to the challenges associated with
507 gaining a full picture of pluvial flooding - which is often localized and fast-developing. This becomes
508 apparent when the inundation extents collated by the EA and Council are compared (Figure 3). Large
509 discrepancy can be noted in places. Furthermore, the accuracy of model prediction can be equally uncertain,
510 due largely to: (i) the quality of the input data, including the representation of spatial and temporal
511 characteristic of precipitation, and topography; and (ii) simplified treatment of infiltration and negligence of
512 flooding from pluvial sources (i.e. drains). Despite the relative small size of the catchment (12 km by 7 km),
513 variability in the spatial and temporal distribution of rainfall is expected. A single rainfall time series
514 immediately adjacent to the study site to the northeast is used in the simulation and it is likely that this has
515 likely introduced some errors to the representation of rainfall, especially in the rural regions to the west. The

516 use of high resolution radar-derived precipitation data might provide a more accurate representation though
517 this is not without its own uncertainties. Uncertainty is also present in the topographical data with a vertical
518 error of +/-15-20 cm in the original LiDAR dataset. Sensitivity to mesh resolution suggests that, although the
519 difference in the total inundated area is similar, the spatial and temporal distribution of the predicted wet area
520 and water depth can vary to a large extent (Figure 4). A similar conclusion can be drawn with regards to the
521 roughness specification (Figure 4) where the model is relatively sensitive to roughness when evaluated
522 against the Fit statistic but less so when evaluated against the total inundation area. Despite this sensitivity,
523 the use of 20 m DTM still captures the spatial dynamics of surface flow routing.

524

525 There are also uncertainties in the process representation. The model assumes runoff due to infiltration
526 excess dominates. Furthermore, surcharge from storm sewers is not considered by the model, but rather, a
527 drainage capacity coefficient is used to represent the effect of drainage. Errors are expected with this
528 approach, particularly at the local scale. The uncertainties involved in the process representation are offset
529 during model calibration, when soil hydraulic conductivity is adjusted aiming to reproduce the observed
530 flooded areas, with a focus on the Derringham Area. It is recognized that soil hydraulic conductivity is a
531 complex coefficient to determine, especially for an urban catchment like West Hull. However, a uniform
532 hydraulic conductivity is used in the simulations and we did not attempt to represent the spatial variation of
533 soil hydraulic conductivity due to the complexity involved in determining K_s for urban catchment and the
534 simplified nature of the model.

535

536 **4.3. Effects of urban and rural drainage and storage capacity**

537 Improvement to urban drainage and storage capacity is regarded as a potential measure to reduce the risks of
538 catastrophic pluvial flood events in Hull (Hull Council 2009). Results suggest that improving drainage and
539 storage capacity indeed could reduce the extent of inundation (Figure 9), but due to the magnitude of the
540 event and the contribution of flood water from rural land, it may not completely drain the excess surface
541 water, even with an increase of capacity to 120 mm/day. Though for localized ponding with no inflow from
542 rural land (e.g. Points 5 and 12) this increase in capacity would be effective. It should be noted that we
543 assume that the drainage system functions throughout a flood event to its full capacity. However, it is

544 possible that in many situations, the actual drainage capacity could be degraded by malfunctioning pumps or
545 blocked drains.

546

547 **4.4 Effect of improved rural land drainage and storage capacity**

548 When the rural land drainage and storage improvement scenarios are investigated, greater sensitivity is noted
549 compared to the urban improvement scenarios, both globally (Figure 13) and at discrete points along the two
550 main flow pathways (Figure 14). Comparing the scenarios of improved rural drainage/storage capacity
551 (Figure 13) with urban drainage/storage scenarios of similar magnitude, it is clear that areas adjacent to the
552 rural parts benefit most from rural intervention. These areas (e.g. Derringham Park, Figure 1) were amongst
553 the worst-hit during the 2007 flood. Mass balance analysis in Figure 9d and Figure 12d suggests that a 10
554 mm improvement in urban areas has a similar effect on water balance as a 20 mm improvement in rural areas.
555 Given the size ratio between the urban and rural areas in this case study (4:1), the rural improvement can be
556 regarded as more effective on a unit area basis. In other words, a 20 mm improvement over one-unit rural
557 area is as effective as a 10 mm improvement over four-unit urban area in reducing surface water for this
558 specific site.

559

560 Furthermore, comparing Figure 10b with Figure 13b, although similar in the capacity to reduce total volume
561 of surface water as shown in Figures 9d and 12d, a 40 mm rural improvement (Figure 13b) is significantly
562 more effective in reducing maximum flood (both depth and extent) than a 20 mm urban improvement
563 (Figure 10b).

564

565 Combining urban land drainage and storage improvement, the water depth can be reduced substantially.
566 However, none of the scenarios could reduce surface runoff completely. This is not surprising when the
567 magnitude of the flood event and the size ratio of rural to urban area (1:4) are considered. It is expected that
568 improved rural land drainage and storage capacity will become more effective for larger catchments and
569 lower-intensity rainfall events.

570

571 **4.5 Process representation**

572 The model treats the drainage capacity using a simplified approach and assumes a uniform mass loss for
573 individual pixels to represent the sewer capacity. A similar method is used by Mignot *et al.* (2006), where
574 drainage capacity is subtracted from the model-derived flow hydrographs in two inlets of an urban site to
575 represent the effect of storm sewer drainage in the upstream of the city. Although the total volume of water
576 lost to storm sewers is expected to be reasonably well represented, the temporal changes in capacity of the
577 storm sewer network at the local scale will be simplified due to the interaction at the surface/sewer
578 boundaries (manholes). Therefore, this may over- or under-estimate the amount of mass loss to the storm
579 sewer systems. Due to the intensity and magnitude of the storm simulated and observations during the flood,
580 the drainage capacity was reached early on in the event. Therefore the simulations may have overestimated
581 the mass loss to storm sewers. Further modifications to the model may use ideas from the rational or Lloyd-
582 Davies equation (Hamill 2010) widely used in the design of storm sewer systems, which takes the form of
583 $Q_p = CiA$, where Q_p is peak discharge to a sewer inlet; A is the catchment area; C is a coefficient of runoff
584 representing the characteristics of the catchment (e.g. impermeability); and i is the rainfall intensity, which is
585 calculated as the average rainfall during the time of concentration, defined as the total time required for rain
586 falling at the catchment boundary to flow to the first sewer and then carried through the sewer system to the
587 design point. The rational method is essentially a lump-model that translates rainfall into runoff based on
588 sub-catchment characteristics while relating rainfall intensity to time of concentration. The effect of
589 coefficient of runoff (C) is represented in this study in a distributed way using the combination of infiltration
590 capacity and evapotranspiration, with the former being related to land uses. Routing runoff explicitly
591 improves the representation of runoff timing. However, the use of drainage capacity on a cell-by-cell basis
592 assumes storm sewer explicitly drains rainfall at every single pixel, whilst in reality, only at certain points
593 (manhole inlets), rainfall-runoff is drained by the sewer system. As a result, overestimation of drainage loss
594 is expected with the current approach as the timing of flow through the system is not considered explicitly.
595 The extent of overestimation depends on the interplay between rainfall intensity, topographic gradient and
596 parameters used in the modelling. However, the loss overestimation should diminish if the simulation is
597 allowed to run long enough as the sewers capture the runoff (e.g. in this case study). An alternative approach
598 to the cell-by-cell representation is to consider the actual locations of manhole inlets and use empirical
599 equations to calculate the amount of water drained at the inlets.

600

601 Finally, we note that the choice of drainage capacity adopted for a particular simulation should correspond to
602 the duration of an event. For shorter duration events, the design standard corresponding to the event duration
603 should be used instead of scaling the daily design standard as it is a parameter that cannot be scaled linearly
604 with time. In this study, we used the daily drainage design standard (70mm/day in Hull) to estimate drainage
605 loss. As the rainfall lasted for most of the day (Figure 2), the daily design capacity is thought to be a valid
606 representation. Further studies could be directed to evaluate alternative approaches to representing storm
607 sewer design capacity, e.g. adopting temporally-varying hourly design capacity according to the rainfall
608 pattern observed in the rainfall hyetograph.

609

610 5. Conclusion

611 This paper presents the application of a simple urban hydro-inundation model, coupling hydrological
612 processes within an inertial-based surface flow routing model. After sensitivity testing and model calibration
613 using the June 2007 flood event occurred in the City of Kingston upon Hull, UK, the application focuses on
614 evaluating the effect of improved drainage and storage capacities at both the urban and rural areas.

615

616 Sensitivity analysis reveals the danger of using a global metric (e.g. inundation extent) to evaluate model
617 sensitivity, as when using inundation extent, we found that the peak inundation varies only marginally.
618 However, a comparison of distributed flood areas show the model is sensitive to both mesh resolution and
619 roughness specification. The results obtained from the combined hydrological/hydraulic modelling
620 complement previous studies on scaling issues in flood inundation modelling (e.g. Yu and Lane 2006a;
621 Ozdemir *et al.* 2013). It is expected that the degree of sensitivity to mesh resolution and roughness is also
622 associated with the topographic characteristic of the study site. With a sloped terrain, the sensitivity will
623 likely be magnified as compared to a mild sloped terrain. The model was calibrated using soil hydraulic
624 conductivity against the reported inundated areas collated from two sources (EA and Hull Council) and the
625 timeline of the event. Results highlight the challenges in validating surface water flood modelling in urban
626 areas. This is primarily due to the nature of surface water induced urban flooding. Such events are often
627 unexpected and sudden in nature, characterised by shallow water depth and local ponding. As this study
628 shows, it is therefore very important to include not only the urban areas but the rural/suburban areas that may
629 contribute to the drainage area and flooding. This study clearly illustrates how the correct parameterisation of

630 infiltration and water loss in the contributing hills west of Hull are vital for successful model performance.
631 Overall, model performance is just as strongly controlled by these rural factors as internal model parameters
632 such as roughness. This serves as an important reminder to researchers simulating urban flooding that it is
633 not just the internal parameterisation that is important, but also to use the correct inputs of water from outside
634 the area of study, the rationale that behind tightly coupling catchment hydrological processes and urban flood
635 inundation.

636

637 Future work should be directed towards obtaining high resolution and good quality observation data for
638 model validation. Calibration also highlights the needs for further improvement of the modelling approach,
639 including improved representation of drainage capacity and precipitation, and improved computational
640 efficiency to allow for finer topographic data to be used in the simulation.

641

642 The scenario-based approach used to evaluate the effect of drainage and storage capacity provides some
643 useful insight into the potential adaptation measures to surface water flooding and their effectiveness. Such
644 measures are often site-specific. This paper used a simplified parameter (i.e. drainage and storage capacity)
645 to represent the bulk effect of improved urban and rural drainage and storage capacities. Improved drainage
646 and storage capacities result in corresponding reductions of flood extent and magnitude as expected.
647 However, none of the scenarios result in complete drainage. Due to the magnitude of the flood event
648 considered and the relative size of the rural areas, the findings are therefore limited to the particular
649 catchment and event. Future studies could be undertaken to evaluate: (i) the impacts of drainage and storage
650 capacity in catchments with varying urban/rural size ratio; (ii) the response of a catchment to precipitation of
651 varying magnitude, and spatiotemporal characteristics; and (iii) the alternative measures to alleviate the
652 potential impacts of surface flood risks.

653

654 **Acknowledgements**

655 The author wishes to thank two anonymous reviewers who provided very useful and constructive comments
656 on the paper. The author also thanks the editors who processed the submission.

ACCEPTED MANUSCRIPT

658 **Reference**

- 659 Aronica, G.T. and Lanza, L.G. 2005. Drainage efficiency in urban areas: a case study. *Hydrological*
660 *Processes*, 19(5):1105-1119.
- 661 Bates, P.D., Horritt, M., and Fewtrell, T. 2010. A simple inertial formulation of the shallow water equations
662 for efficient two-dimensional flood inundation modelling. *Journal of Hydrology*, 387(1-2): 33-45.
- 663 Blanc, J., Arthur, S., Wright, G. and Beevers, L. 2012. *Natural flood management (NFM) knowledge system:*
664 *Part 3 - The effect of land drainage on flood risk and farming practice. Scotland's Centre of Expertise*
665 *for Waters, final report*, 38pp.
- 666 Calder, I.R., Harding, R.J. and Rosier, P.T.W. 1983. An objective assessment of soil moisture deficit models.
667 *Journal of Hydrology*, 60: 329-355.
- 668 Casas, A., Lane, S.N., Yu, D. and Benito, G. 2010. A method for parameterising roughness and topographic
669 sub-grid effects in hydraulic modelling from LiDAR data. *Hydrology and Earth System Sciences*, 14(8):
670 1567-1579.
- 671 Chen, A.S., Djordjević, S., Leandro, J. and Savić, D., 2007. The urban inundation model with bidirectional
672 flow interaction between 2D overland surface and 1D sewer networks, NOVATECH 2007, Lyon,
673 France, pp. 465-472.
- 674 Chen, A.S., Djordjević, S., Fowler, H.J., Burton, A., Walsh, C., Harvey, H., Hall, J., Dawson, R. and Wood,
675 G. 2009. Pluvial flood modelling of the South East London Resilience Zone in the community
676 Resilience to Extreme Weather (CREW) Project. 44th Flood and Coastal Risk Management Conference
677 2009, Telford, UK.
- 678 Coulthard, T.J. and Frostick, L.E. 2010. The Hull floods of 2007: implications for the governance and
679 management of urban drainage systems. *Journal of Flood Risk Management*, 1-9.
- 680 Coulthard T.J., Frostick, L.E., Hardcastle, H., Jones, K., Rogers, D. and Scott, M. 2007a. *The 2007 floods in*
681 *Hull: Interim Report by the Independent Review Body*. Hull City Council, 36pp.
- 682 Coulthard T.J., Frostick, L.E., Hardcastle, H., Jones, K., Rogers, D., Scott, M. and Bankoff, G. 2007b. The
683 2007 floods in Hull: *Final Report by the Independent Review Body*. Hull City Council, 68pp.
- 684 Djordjević, S., Ivetić, M., Maksimović, C., and Rajcević, A. 1991. An approach to the simulation of street
685 flooding in the modeling of surcharged flow in storm sewers. *Proceedings: New Technologies in Urban*
686 *Drainage UDT*, Maksimovic, Editor, Elsevier Publishers, 101-108.
- 687 Environment Agency UK, 2013. What is the updated Flood Map for Surface Water?
- 688 Fewtrell, T.J., Duncan, A., Sampson, C., Neal, J.C. and Bates, P.D. 2011. Benchmarking urban flood models
689 of varying complexity and scale using high resolution terrestrial LiDAR data. *Physics and Chemistry of*
690 *the Earth*, 36: 281-291.
- 691 Hamill, L. 2010. Understanding hydraulics, 3rd edition. Palgrave and Macmillan. pp631.
- 692 Hanna, E., Mayes, J., Beswick, M., Prior, J. and Wood, L. 2008. An analysis of the extreme rainfall in
693 Yorkshire, June 2007, and its rarity. *Weather*, 63(9):253-260.
- 694 Hsu, M.H., Chen, S.H., and Chang, T.J. 2000. Inundation simulation for urban drainage basin with storm
695 sewer system. *Journal of Hydrology*, 234, 21-37.

- 696 Hull Council. 2009. *Surface Water Management Plan and Aqua Green Project*. 72pp.
- 697 Lane, S.N., Reid, S.C., Tayefi, V., Yu, D., Hardy, R.J. 2008. Reconceptualising coarse sediment delivery
698 problems in rivers as catchment-scale and diffuse. *Geomorphology*, 98(34): 227-249.
- 699 Liu, L, Liu, Y, Wang, X, Yu, D, Liu, K, Huang, H, Hu, G (2014) Developing an effective 2-D urban flood
700 inundation model for city emergency management based on cellular automata, *Nat. Hazards Earth Syst.*
701 *Sci. Discuss*, 2, pp.6173-6199.
- 702 Mark, O., Weesakul, S., Apirumanekul, C., Aroonnet, S.B., and Djordjević, S. 2004. Potential and
703 limitations of 1D modelling of urban flooding. *Journal of Hydrology*, 299(3-4): 284-299.
- 704 Mignot, E., Paquier, A. and Haider, S. 2006. Modelling floods in a dense urban area using 2D shallow water
705 equations. *Journal of Hydrology*, 327:186-199.
- 706 Oosterbaan, R.J. and Nijland H.J. 1994. Determining the saturated hydraulic conductivity. Chapter 12: In
707 Ritzema, H.P. (Ed.), *Drainage Principles and Applications*. International Institute for Land Reclamation
708 and Improvement (ILRI), Publication 16, second revised edition, Wageningen, The Netherlands.
- 709 O'Donnell, K.E., Freestone, S.E., Brown, S.E. 2004. *Geochemical baseline data for the urban area of*
710 *Kingston-upon-Hull*. Urban Geoscience and Geological Hazards Programme, Internal Report IR/02/08.
711 British Geological Survey, 61pp.
- 712 Ozdemir, H., Sampson, C., de Almeida, Gustavo A.M. and Bates, P.D. 2013. Evaluating scale and roughness
713 effects in urban flood modelling using terrestrial LIDAR data. *Hydrology and Earth System*
714 *Sciences*, 10: 5903-5942.
- 715 Robinson, M. 1990. Impact of land drainage on river flows. Institute of Hydrology, Wallingford, UK.
716 233pp.s
- 717 Schmitt, T.G., Thomas, M. and Ettrich, N. 2004. Analysis and modelling of flooding in urban drainage
718 systems. *Journal of Hydrology*, 299(3-4): 300-311.
- 719 Sampson, C., Bates, P.B., Neal, J.C. and Horritt, M.S. 2013. An automated routing methodology to enable
720 direct rainfall in high resolution shallow water models. *Hydrological Processes*, 27: 467-476.
- 721 Seyoum, S.D., Vojinovic Z., Price R.K. and Weesakul S. 2012. Coupled 1D and Noninertia 2D Flood
722 Inundation Model for Simulation of Urban Flooding. *Journal of Hydraulic Engineering*, 138: 23-24.
- 723 Tayefi, V., Lane, S.N., Hardy, R.J. and Yu, D. 2007. A comparison of one- and two-dimensional approaches
724 to modelling flood inundation over complex upland floodplains. *Hydrological Processes*, 21(23): 3190-
725 3202.
- 726 Trafford. B.D. 1971 Agricultural land drainage. Welsh Soils Discussion Group Report 12: 68-84.
- 727 Yin, J., Yu, D., Yin, Z.E., Wang, J. and Xu, S.Y. 2013. Modelling the combined impacts of sea-level rise and
728 land subsidence on storm tides induced flooding of the Huangpu River in Shanghai, China. *Climatic*
729 *Change*, 119(3-4): 919-932.
- 730 Yu, D. 2005. *Two-dimensional diffusion wave modelling of structurally complex floodplains*, Ph.D Thesis,
731 School of Geography, University of Leeds, U.K.
- 732 Yu, D. and Lane S.N. 2006a. Urban fluvial flood modelling using a two-dimensional diffusion wave
733 treatment, part 1: mesh resolution effects. *Hydrological Processes*, 20(7): 1541-1565.

- 734 Yu, D. and Lane S.N. 2006b. Urban fluvial flood modelling using a two-dimensional diffusion wave
735 treatment, part 2: development of a sub grid-scale treatment. *Hydrological Processes*, 20(7): 1567-1583.
- 736 Yu, D. 2010. Parallelization of a two-dimensional flood inundation model based on domain
737 decomposition. *Environmental Modelling and Software*, 25(8): 935-945.
- 738 Yu, D. and Lane S.N. 2011. Interaction between subgrid-scale resolution, feature representation and grid-
739 scale resolution in flood inundation modelling. *Hydrological Processes*, 25(1): 36-53.
- 740

ACCEPTED MANUSCRIPT

741

742 List of tables

743 Table 1: Baseline simulation and scenarios with various urban and rural drainage and storage capacities.

Scenarios	Urban drainage and storage capacity (UD) (mm per day)	Rural drainage and storage capacity (RD) (mm per day)
A: Base simulation, assuming urban storm sewer system functions at its full capacity (70 mm/day) and the rural land drainage and storage has a capacity of 15 mm/day during the event.	70	15
B: Improved drainage and storage capacity in urban areas (e.g. engineering measures; swales and balancing ponds).	80	15
	90	15
	100	15
	110	15
	120	15
C: Improved rural land drainage and storage capacity (e.g. land management; flow interceptors and storage areas).	70	35
	70	55
	70	75
	70	95
	70	115
D: Combined BandC	100	75
	120	115

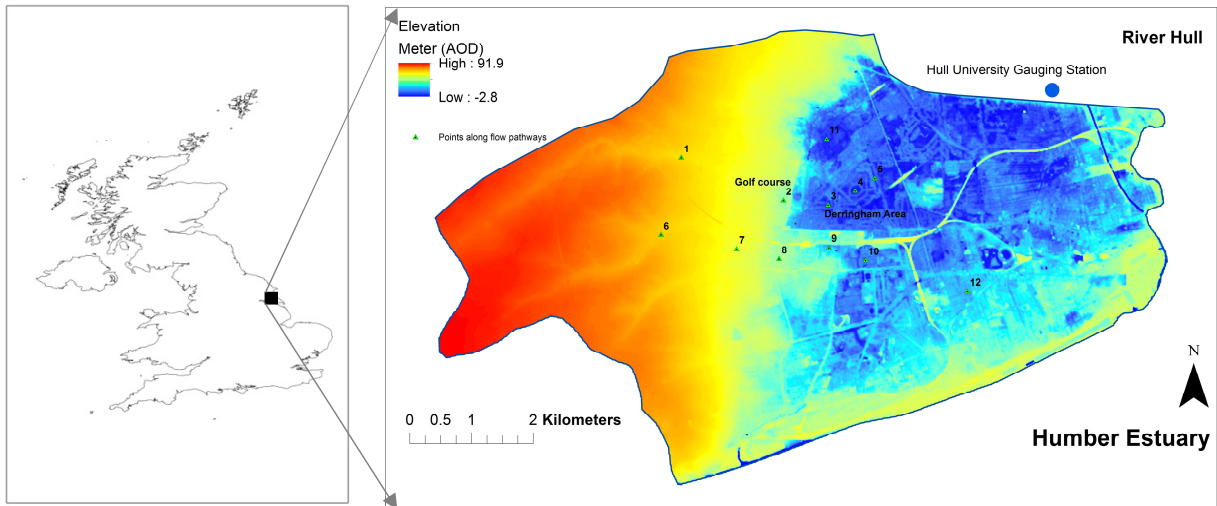
744

745

746

747 List of figures

748

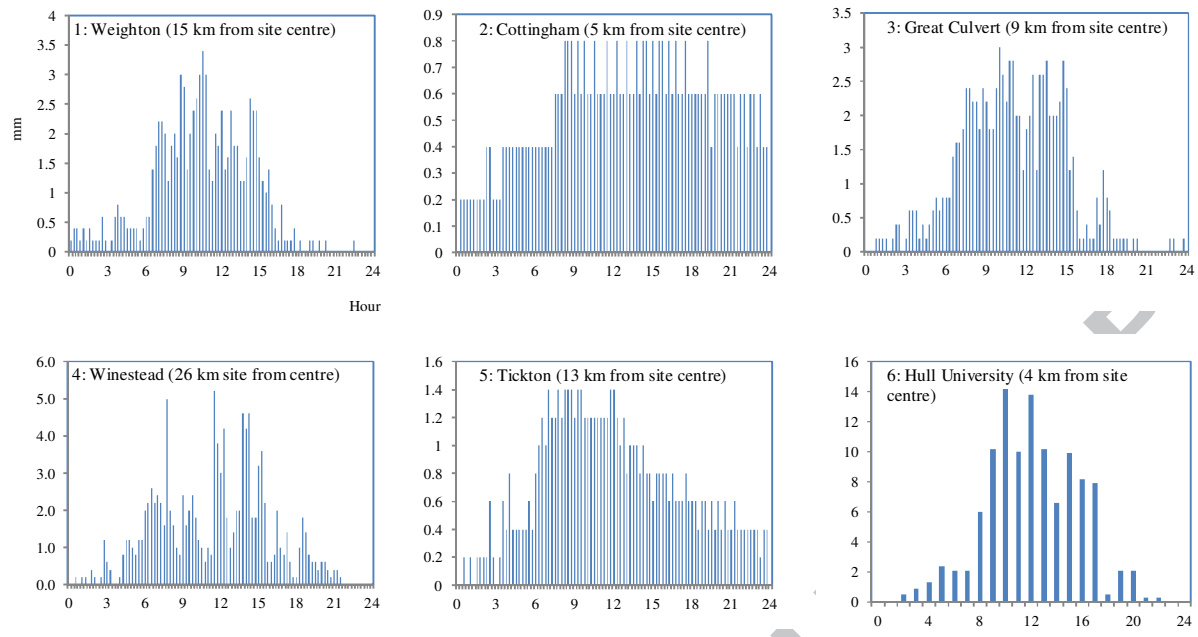


749 Figure 1: Digital Elevation Model of the West part of the City of Kingston upon Hull, UK and contributing catchment

750 areas. Points are locations where the depths are analysed.

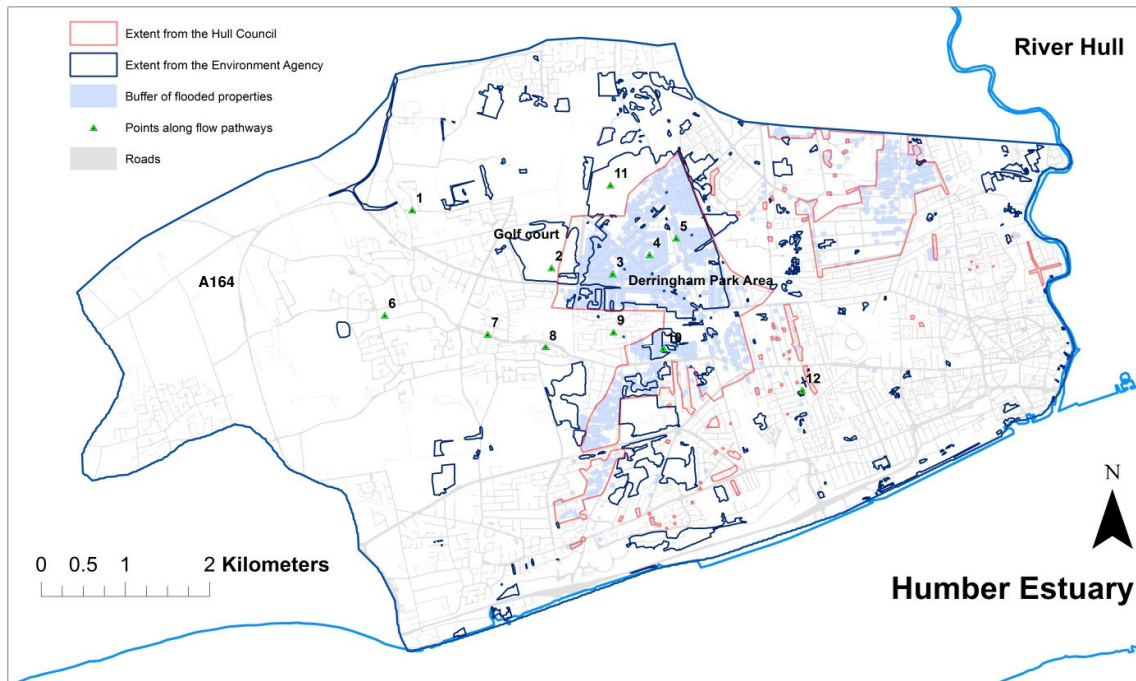
751

ACCEPTED MANUSCRIPT



752 Figure 2: Rainfall hyetographs recorded at the gauging stations in and around the city. Unit: mm/15 minutes for sites 1-
 753 5; mm/h for site 6.

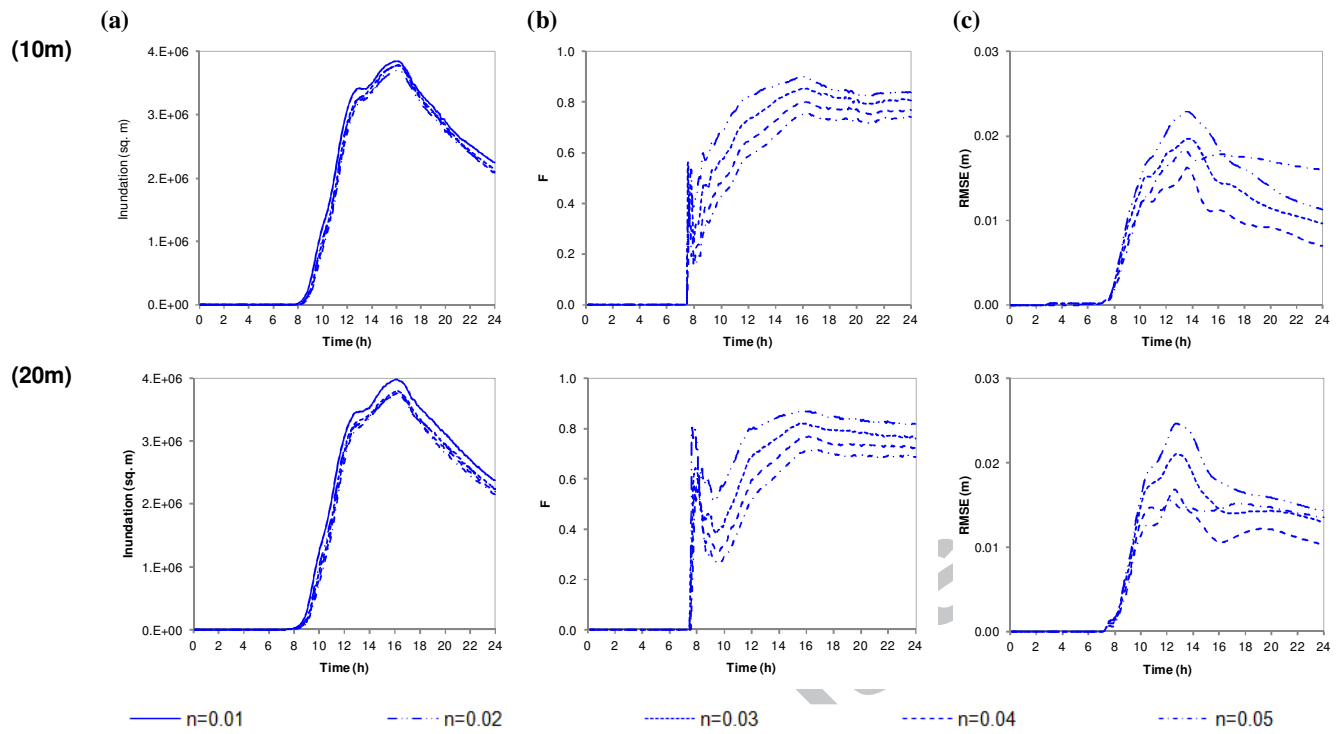
754



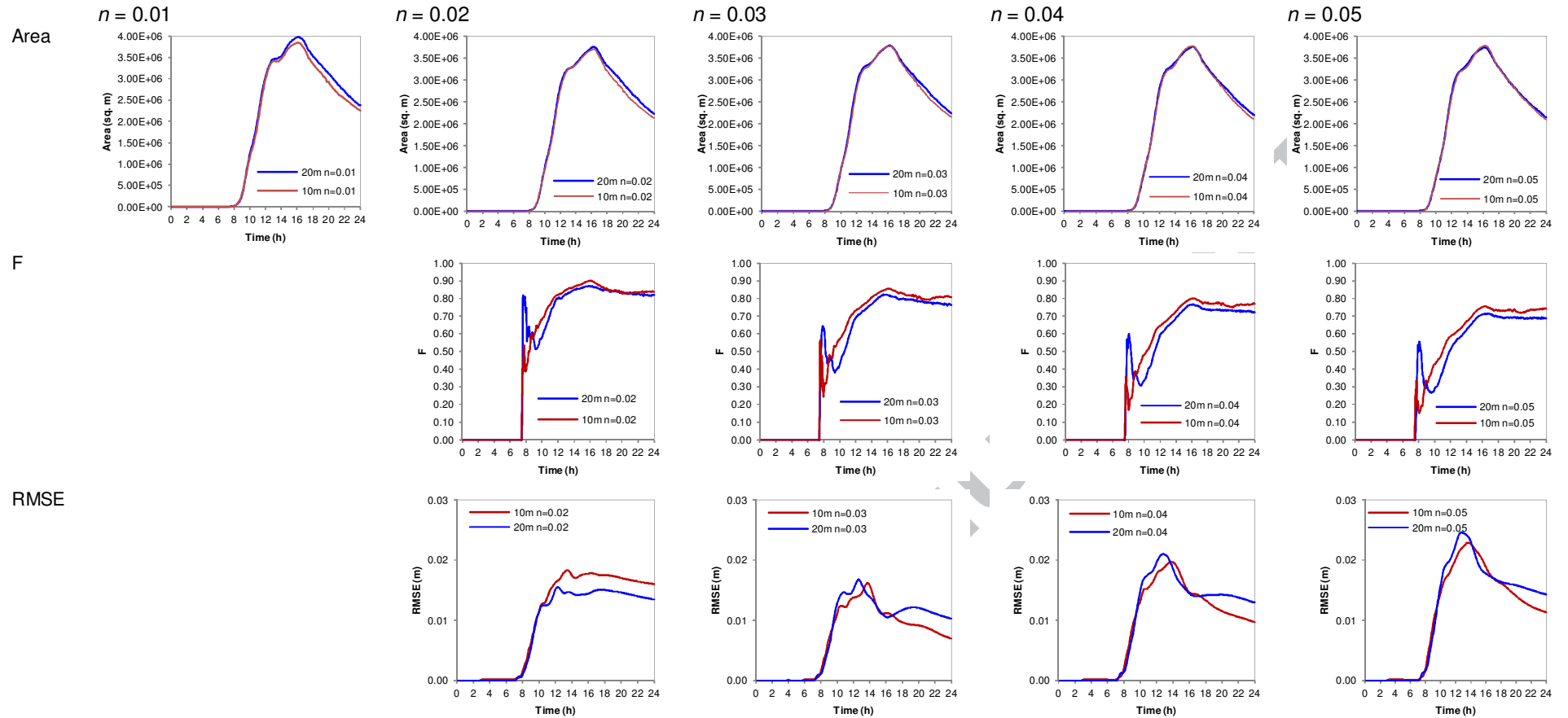
755
756
757

Figure 3: Inundation extent derived from ground survey and aerial photos (UK Environment Agency and Hull City Council); and buffer of properties flooded (Hull City Council).

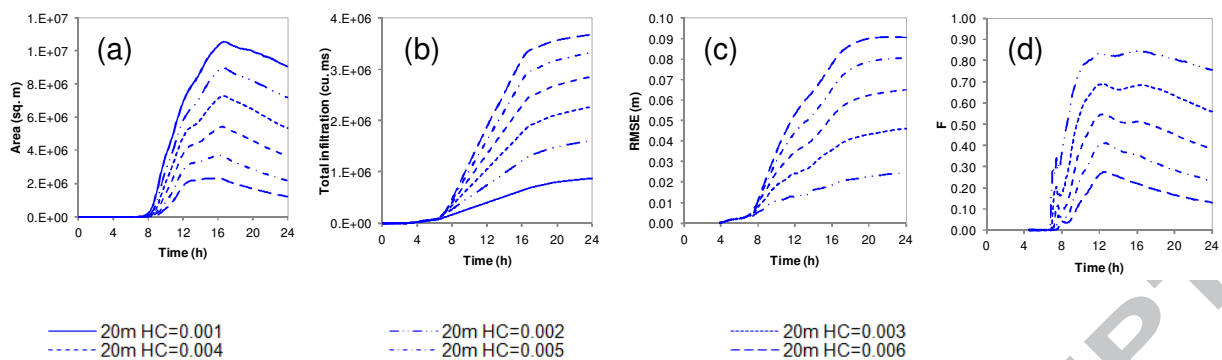
ACCEPTED MANUSCRIPT



758 Figure 4: Sensitivity analysis to mesh resolution and roughness.
 759

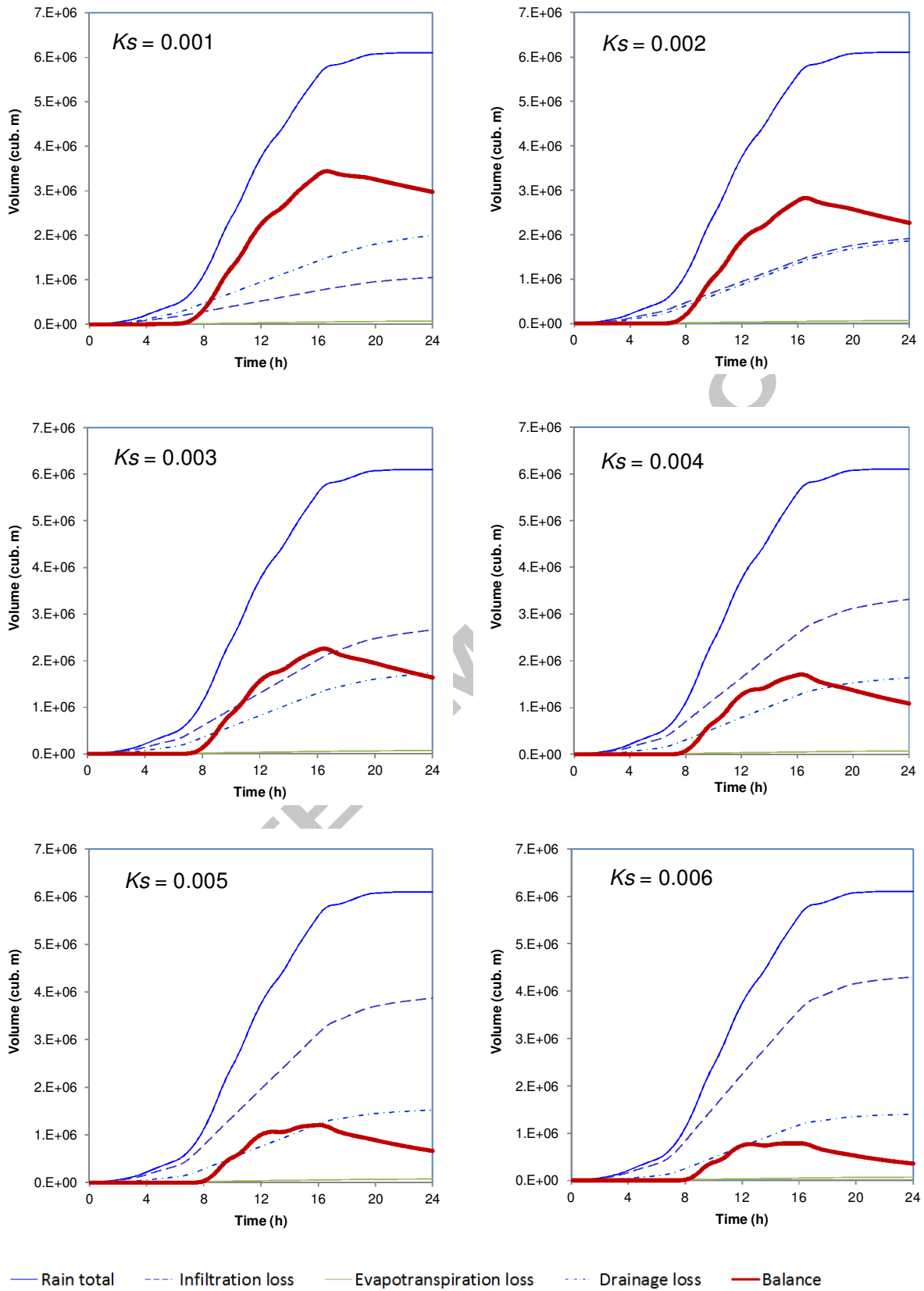


760 Figure 5: Model sensitivity to mesh resolution for different roughness values.



761 Figure 6: Sensitivity analysis to hydraulic conductivity.

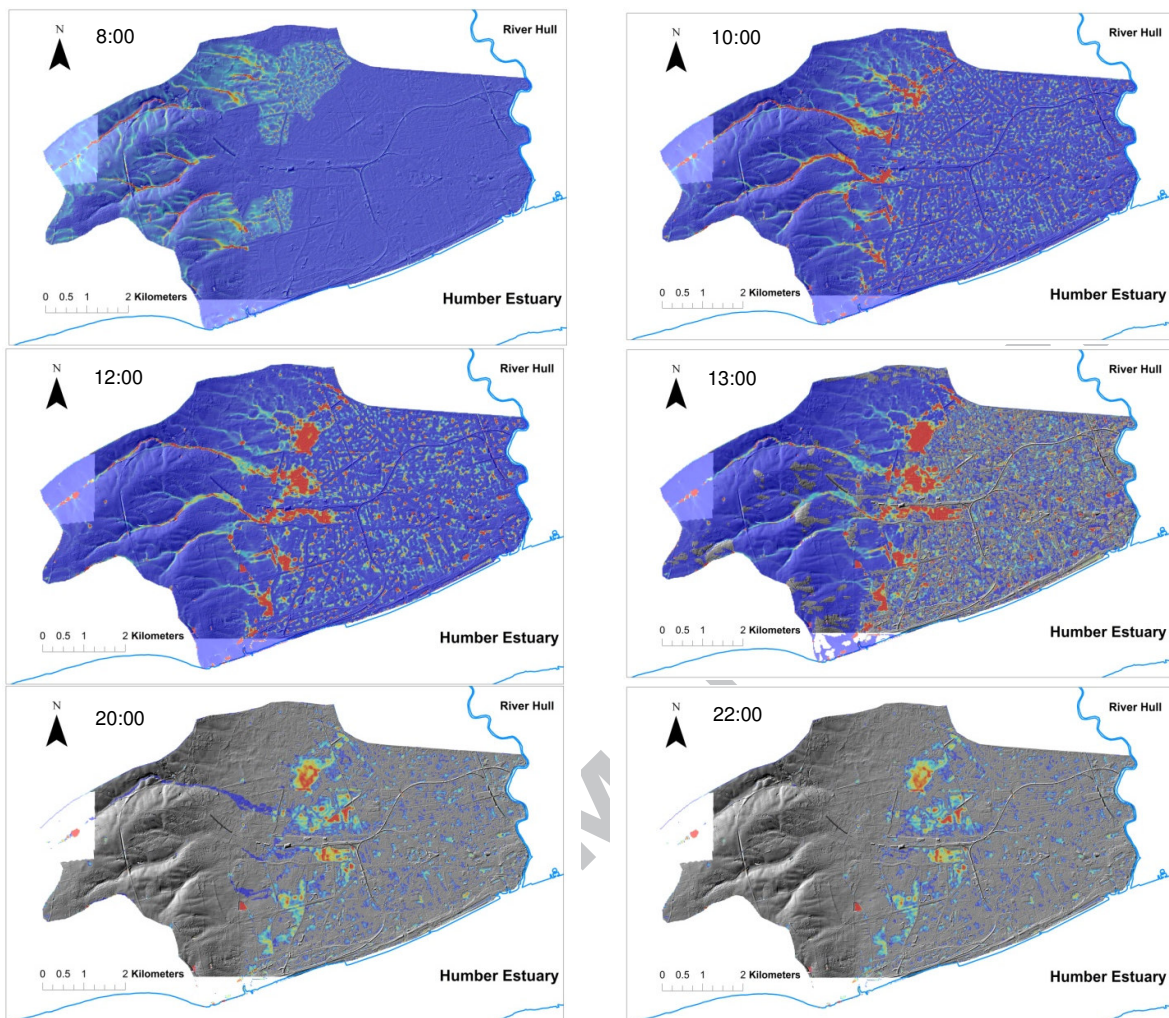
762



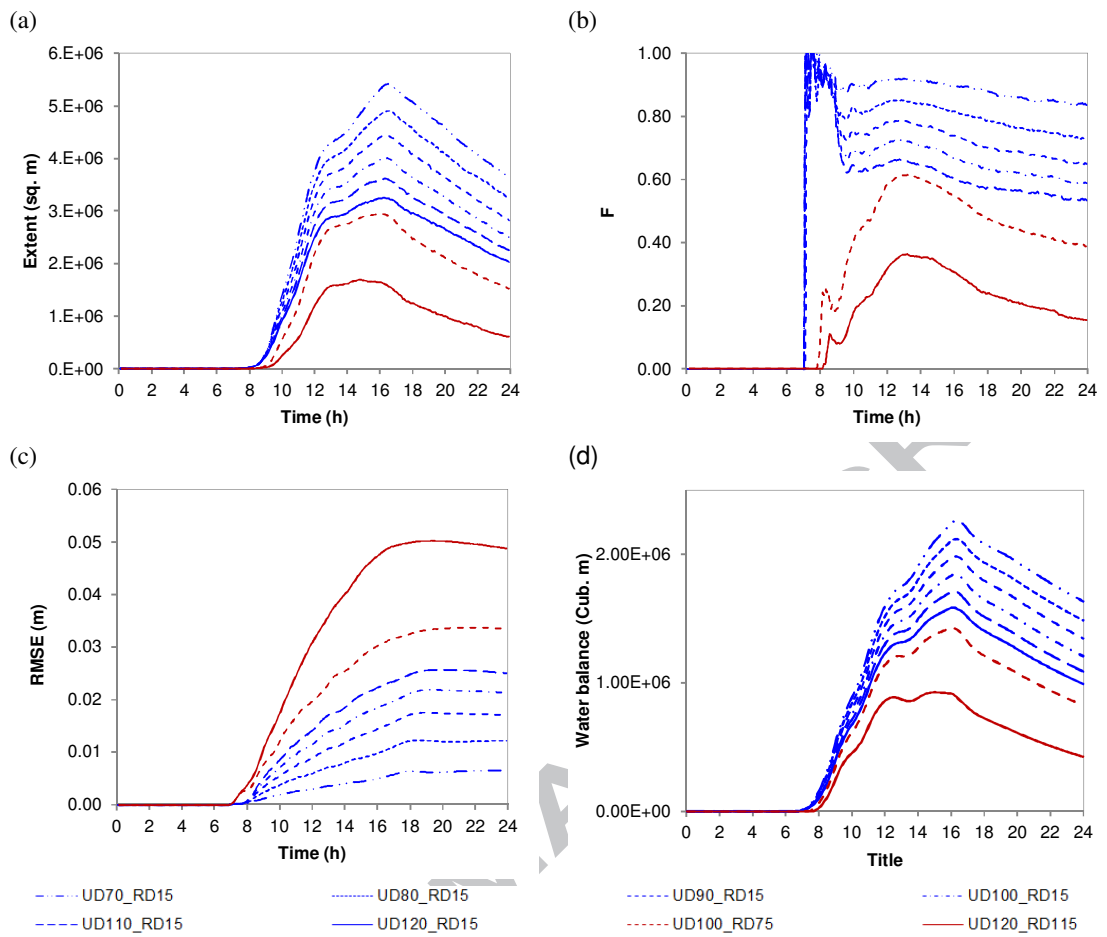
763 Figure 7: mass balance for simulations with different K_s values.

764

765



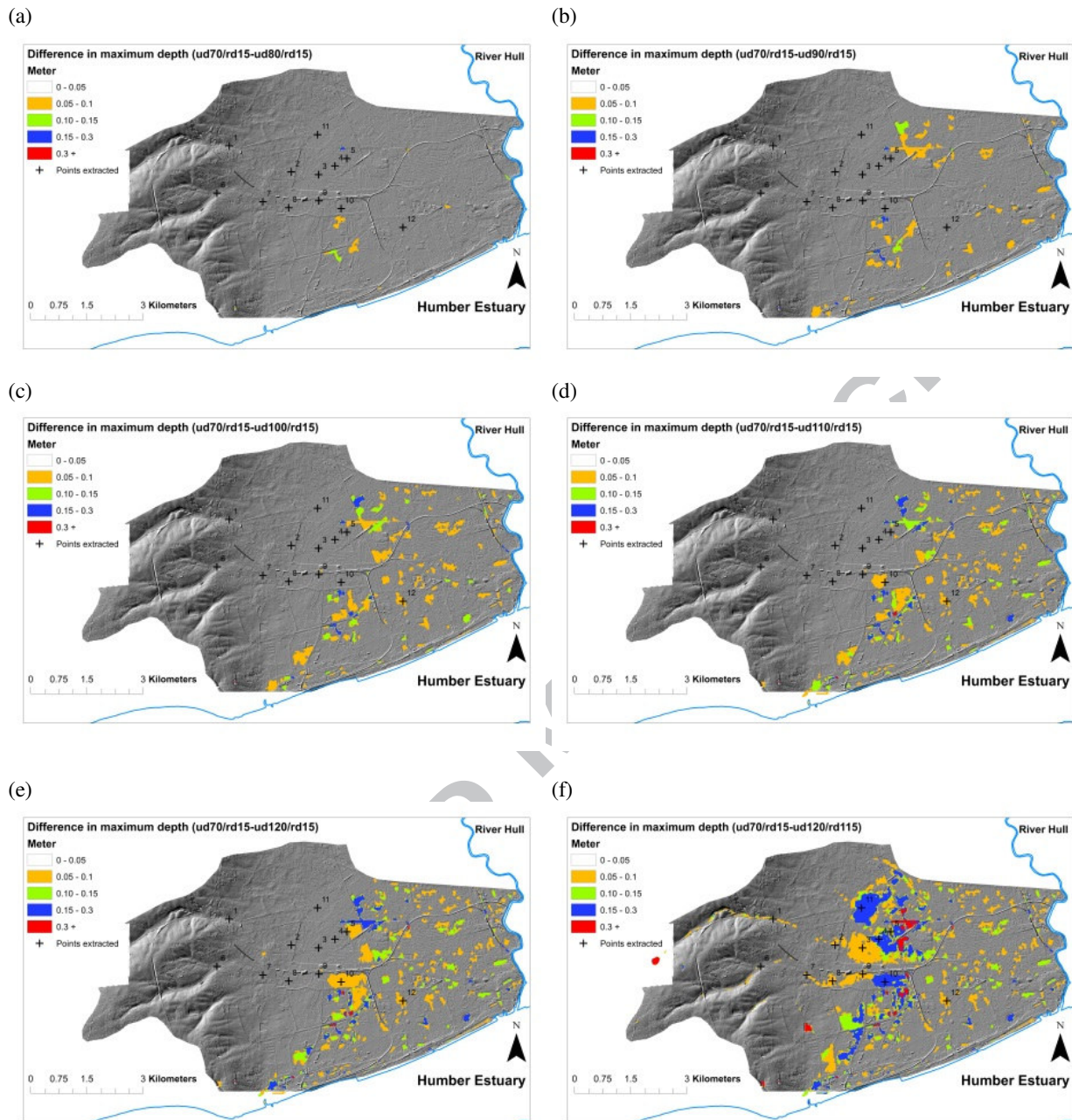
766 Figure 8: Time series of inundation over the study area.
767



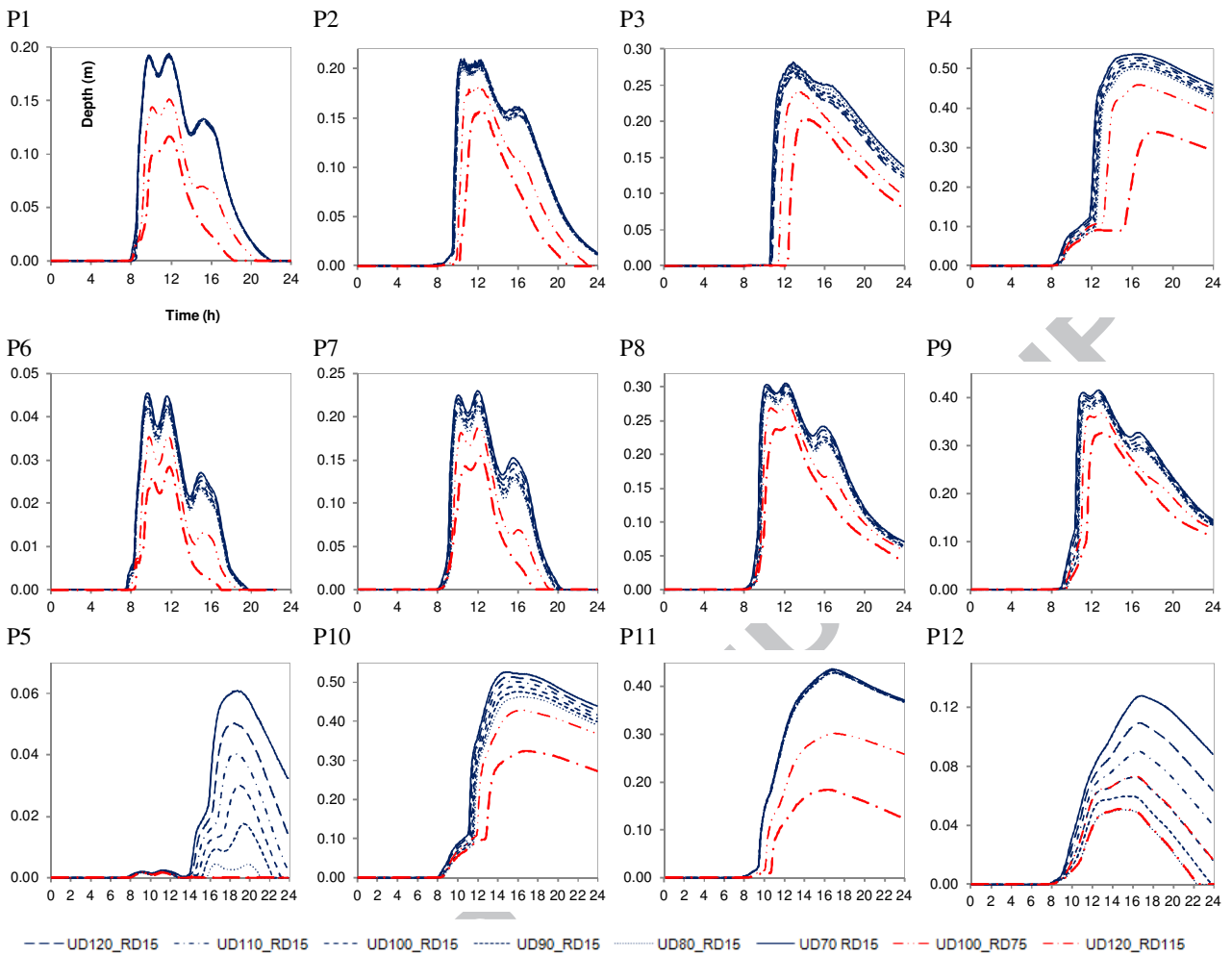
768
769
770
771

Figure 9: Impacts of improved urban drainage capacity scenarios: (a) total inundated areas; (b) F statistics compared to the base simulation (UD70/RD15); (c) RMSE compared to the base simulation (UD70/RD15); and (d) water balance for each simulation.

772

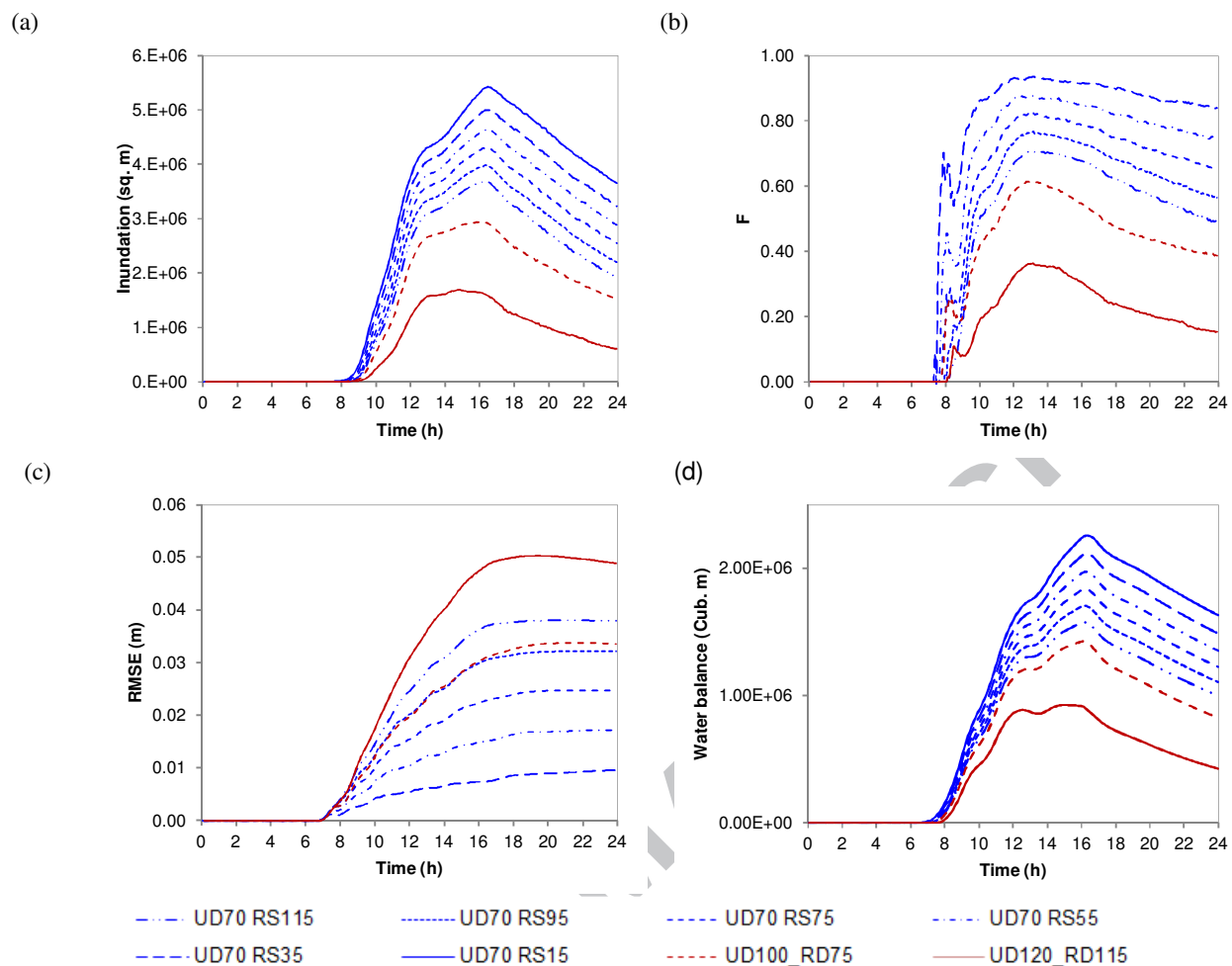


773 Figure 10: Predicted maximum water depth of the simulations with a 70 mm/day (a) and 120 mm/day (b) urban
 774 drainage capacity. Difference in the maximum water depth between the default simulation, and simulations with an
 775 improved urban drainage capacity of 120 mm/day (c).
 776
 777

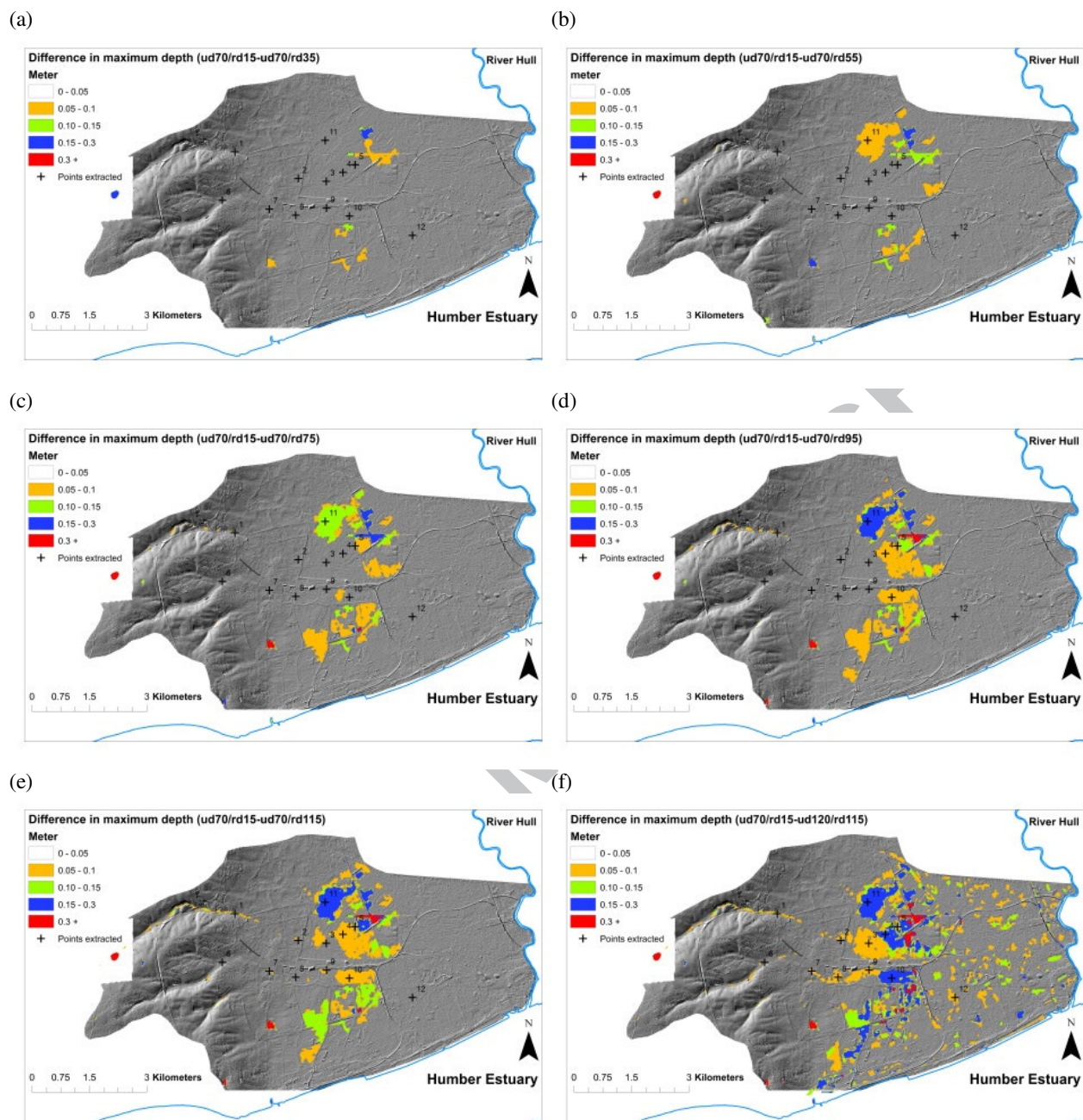


778
779
780

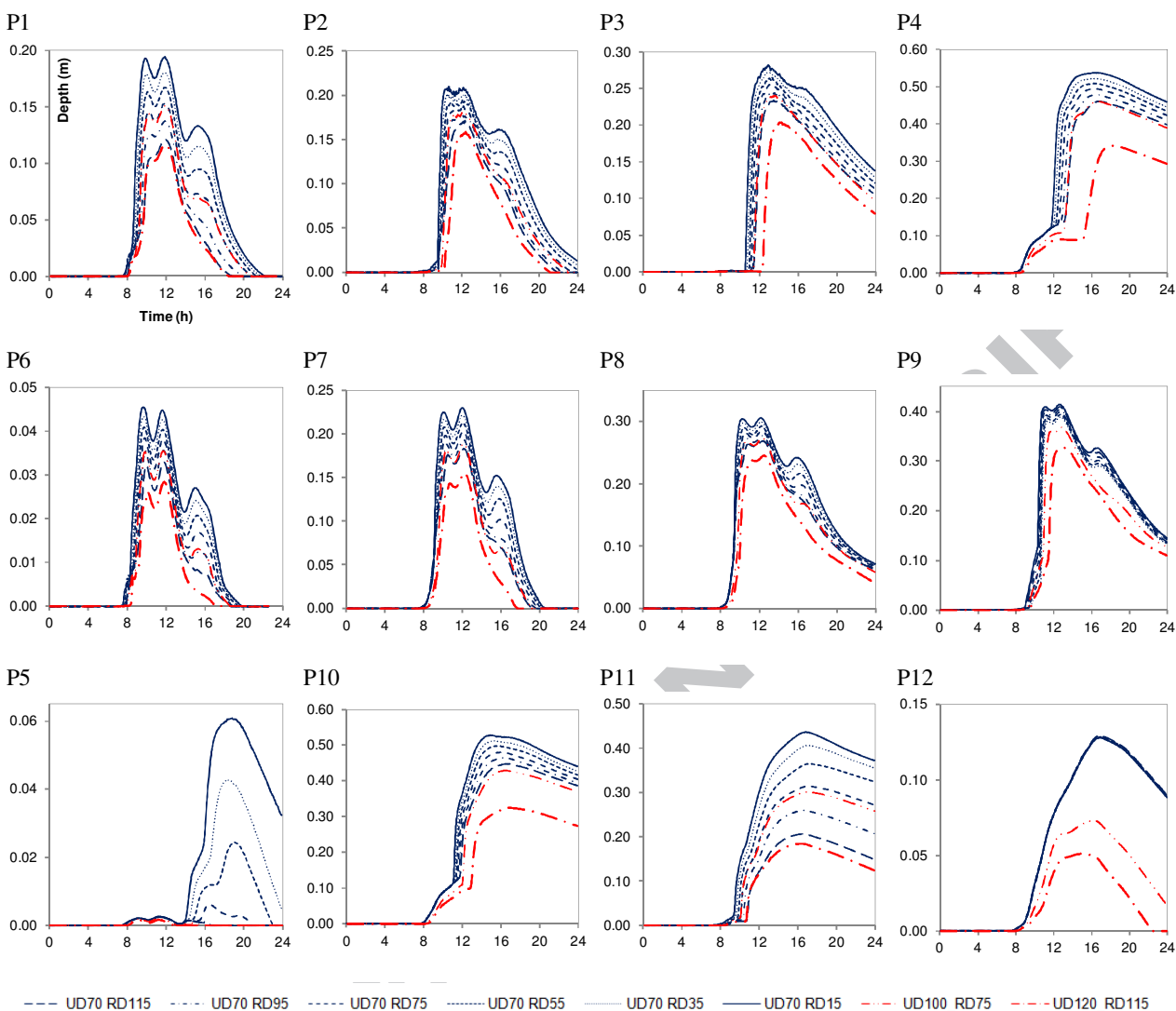
Figure 11: Time series of water depths under urban drainage/storage improvement scenarios along two flow paths (Figure 3) and at local points.



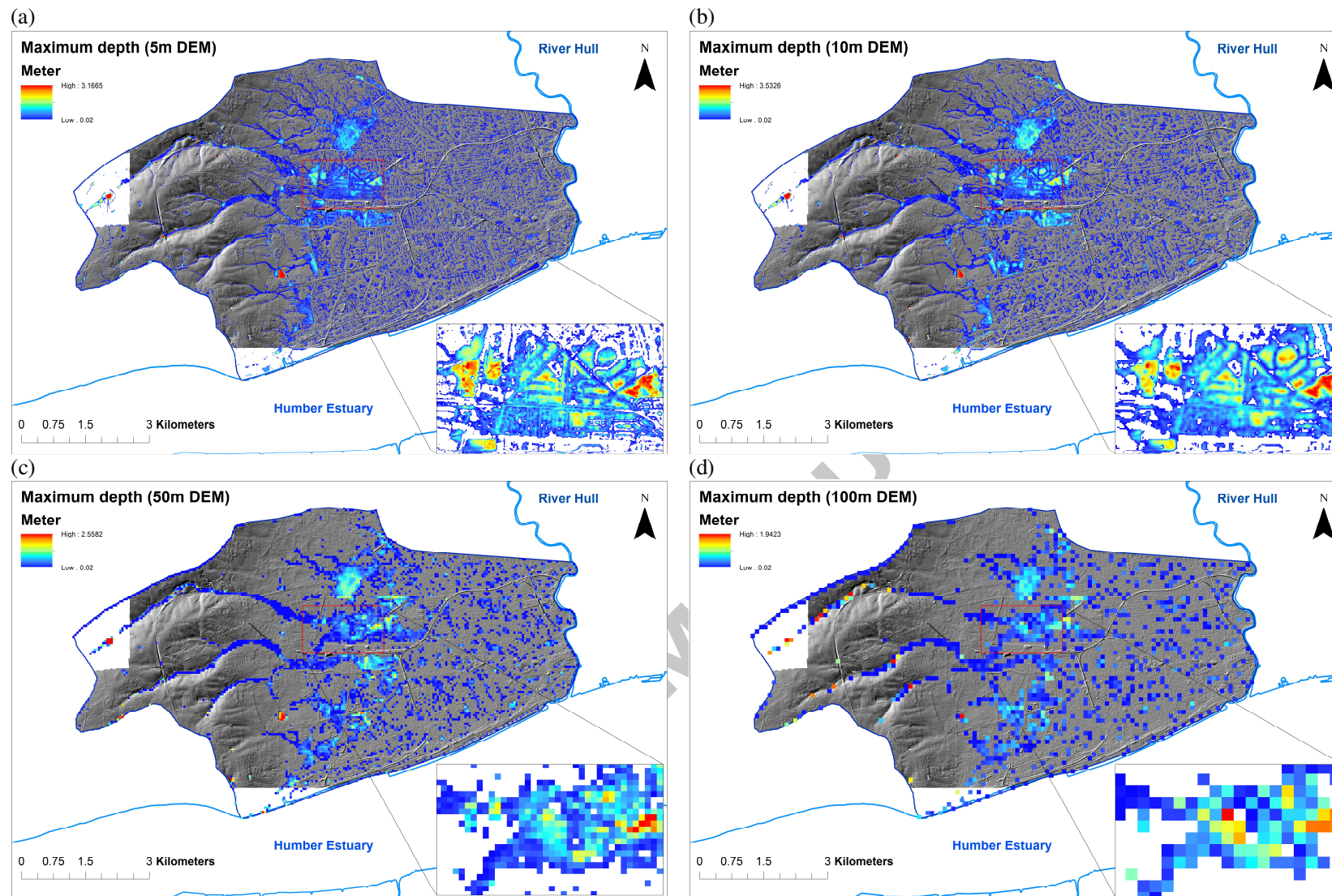
781 Figure 12: Impacts of improved rural land drainage and storage scenarios through land management: (a) total inundated
 782 areas; (b) F statistics compared to the base simulation (UD70/RD15); (c) RMSE compared to the base simulation
 783 (UD70/RD15); and (d) water balance for each simulation.
 784



785 Figure 13: Difference in the maximum water depth predicted between the default simulation and the scenarios with
 786 improved rural drainage capacity: (a) 55 mm/day; and (b) 115 mm/day.
 787



788 Figure 14: Time series of water depths under rural land management scenarios along two flow paths (Figure 3).



789 Figure 15: Effects of model resolution: (a) 5 m DTM; (b) 10 m DTM; (c) 50 m DTM, and (d) 100 m DTM.

790

- 791 1. We modelled a surface flood event due to extreme rainfall with a hydro-inundation model.
792 2. The interaction between surface runoff and sewer surcharge is simplified.
793 3. The model is suitable for pluvial flooding dominated by direct surface runoff.
794 4. Drainage and storage improvement scenarios are evaluated.
795 5. A good level of agreement is reached in model evaluation using observation data.
796

ACCEPTED MANUSCRIPT